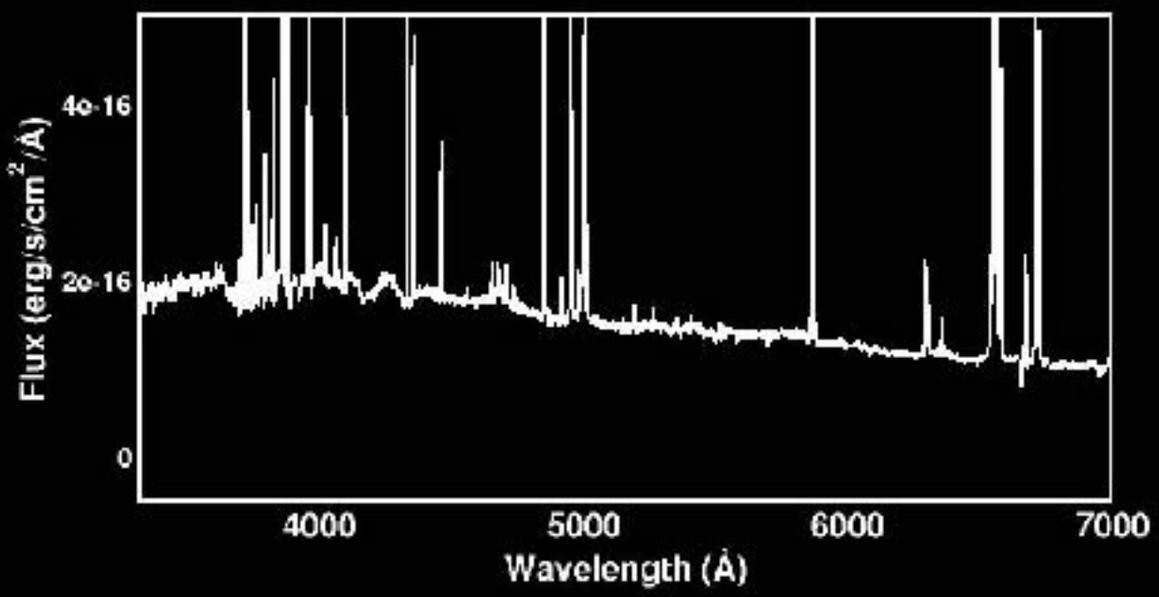
Advances in the study of the softness diagram in the optical and the infrared

Enrique Pérez-Montero
Instituto de Astrofísica de Andalucía - CSIC

In collaboration with:
J.M. Vílchez (IAA), B. Pérez-Díaz (IAA), J.A. Fernández-Ontiveros (CEFCA), C. Kehrig (IAA),

FUNCTIONAL PARAMETERS





Metallicity
(Z)

(i.e. density of elements heavier than H and He)

Ionization parameter
(U)

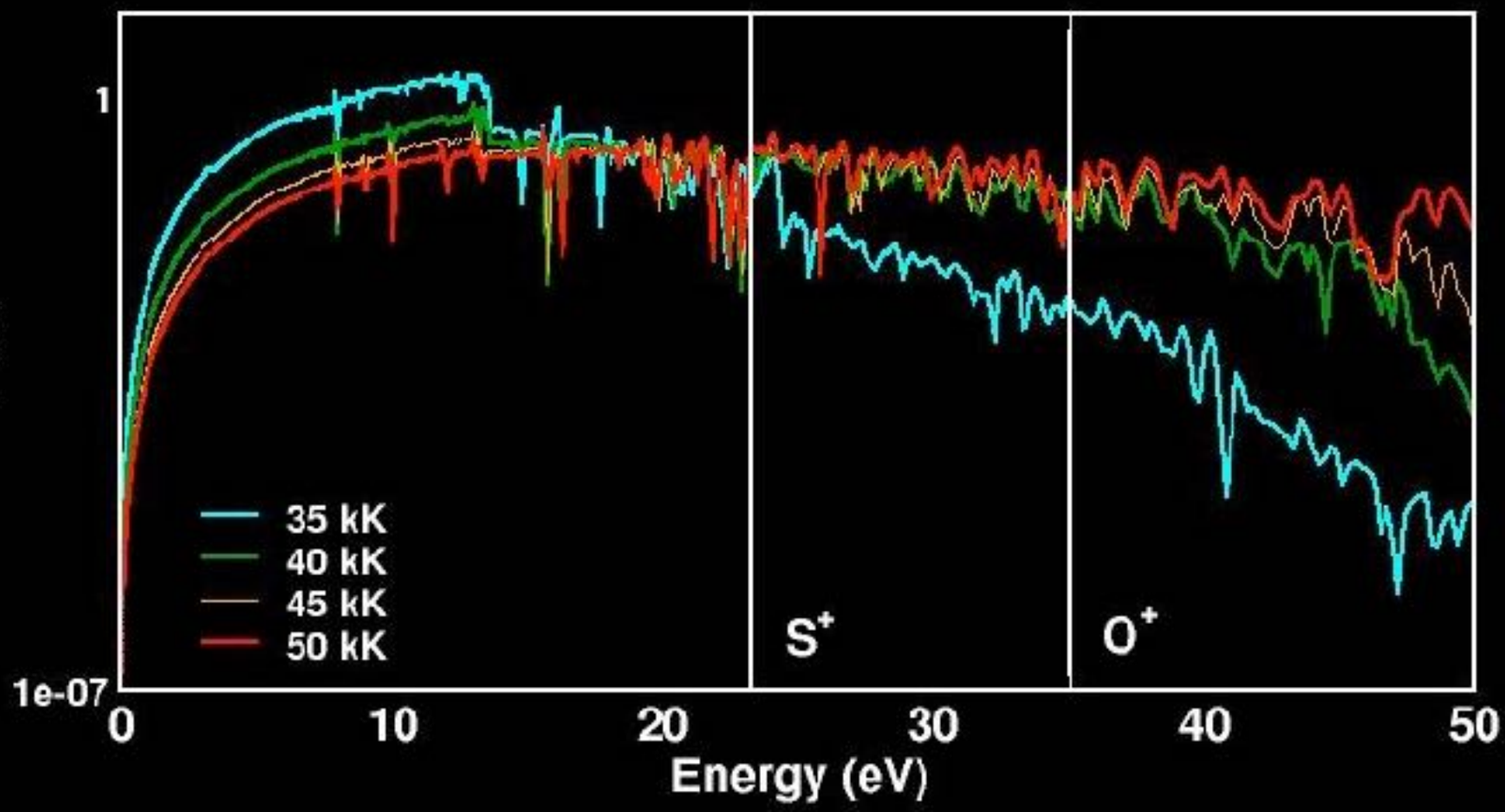
(i.e. ratio between ionizing photons and particles)

Effective equivalent temperature
(T_*)

(i.e. the shape of the ionizing SED)

THE "SOFTNESS" PARAMETER

WM-Basic, log(g)=4.0, [Z] = -0.3



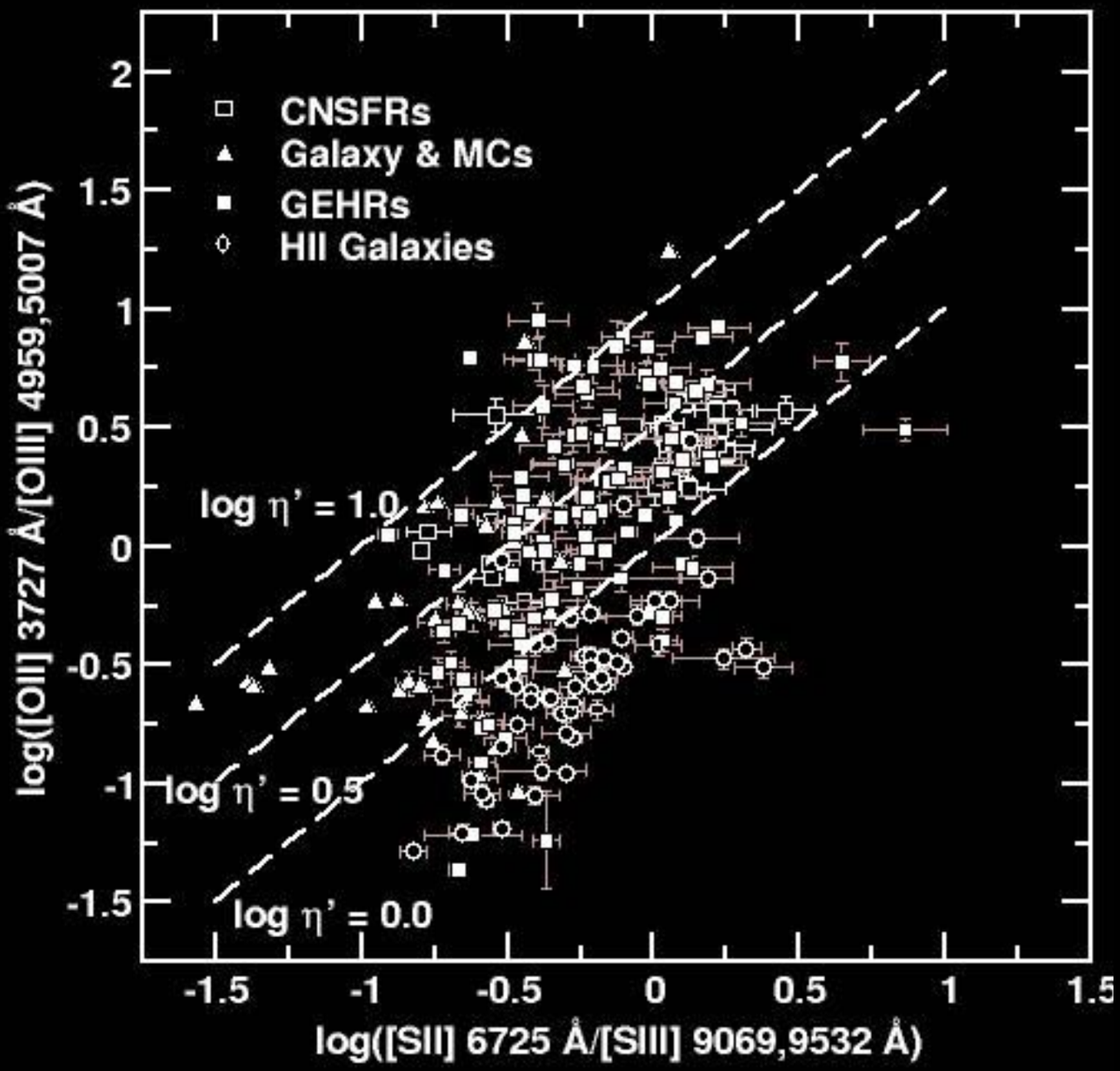
$$\eta = \frac{O^+/O^{2+}}{S^+/S^{2+}} = \frac{[OII]/[OIII]}{[SII]/[SIII]} + o(Z) \propto \frac{Q(O^+)}{Q(S^+)}$$

Vílchez & Pagel (1988)

THE "SOFTNESS" DIAGRAM

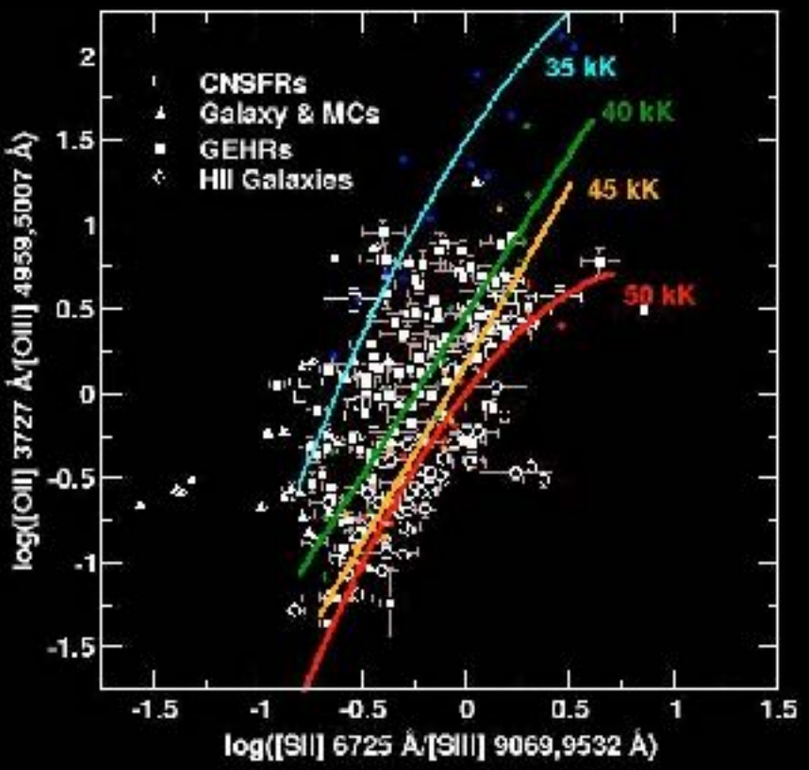
Higher values of η' lead to lower values of T*

CNSFRs and HII galaxies have the largest relative values of T* in YMSCs

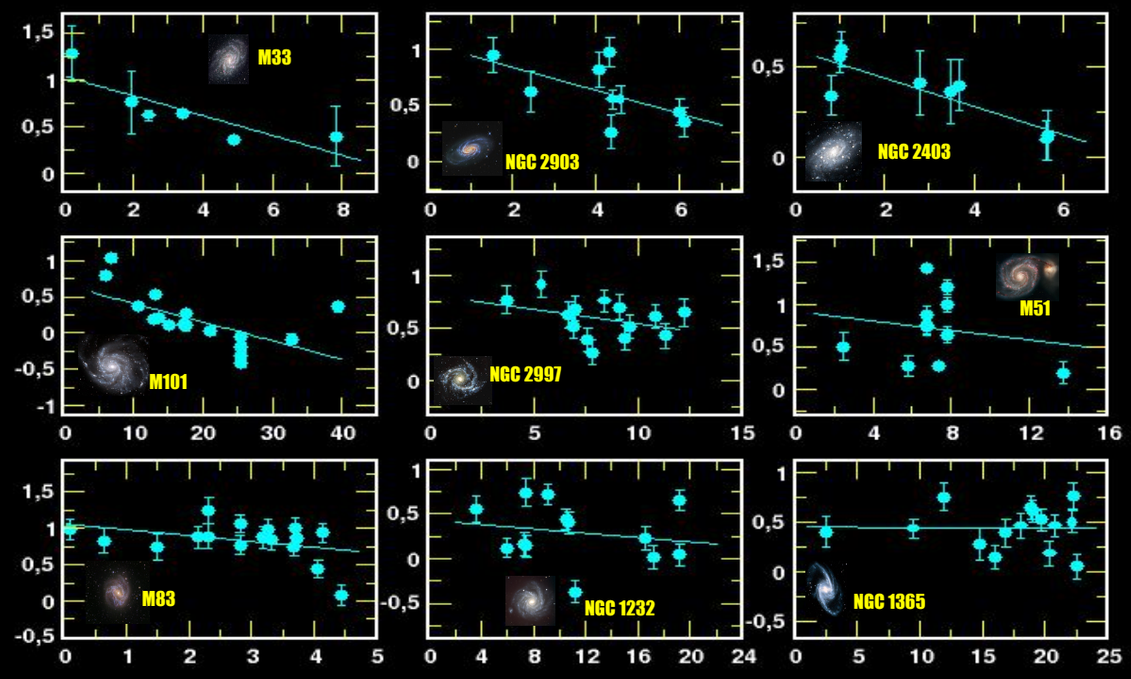


Pérez-Montero & Vílchez (2009)

THE "SOFTNESS" DIAGRAM



WMBasic model stellar atmospheres

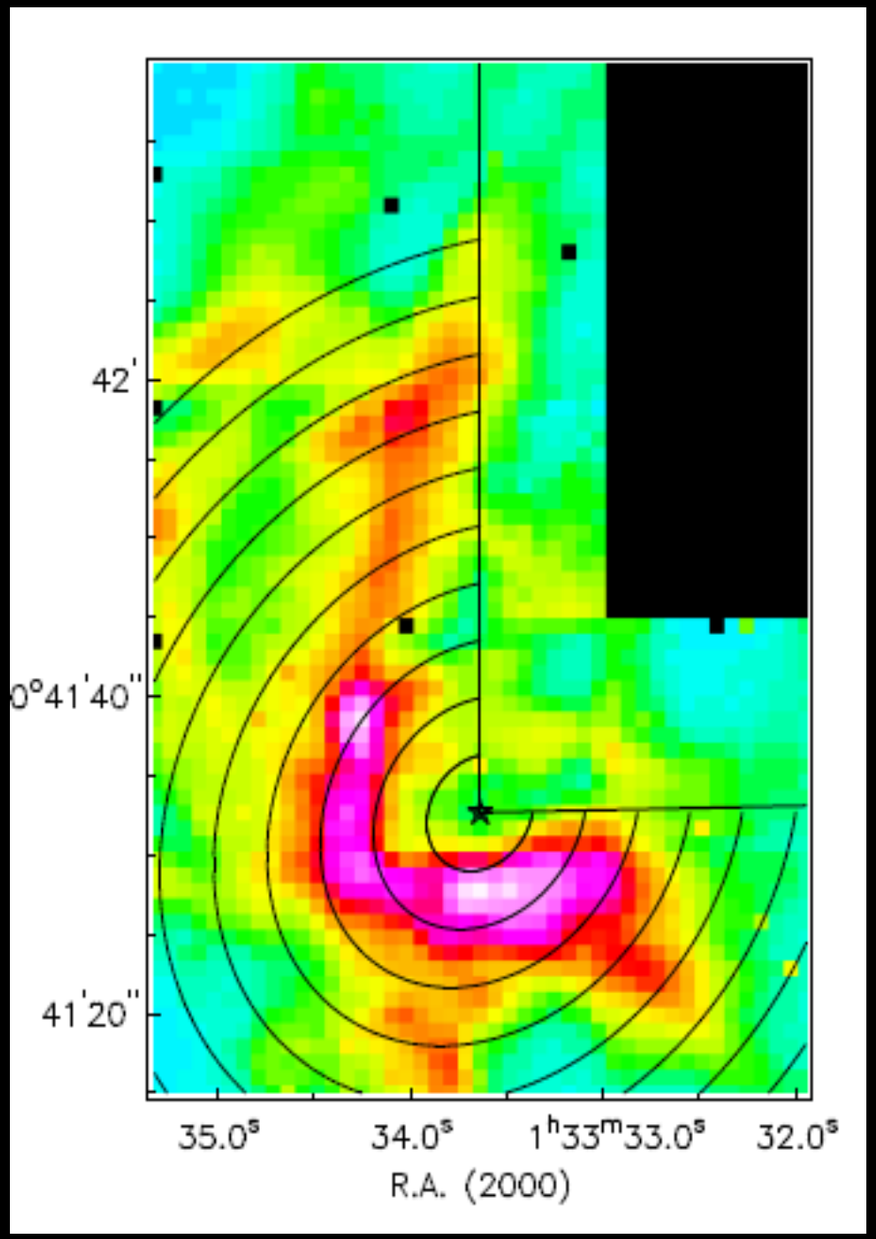


Pérez-Montero & Vílchez (2009)

Photoionization models confirm the relation between η' and the effective temperature of the ionizing source ....

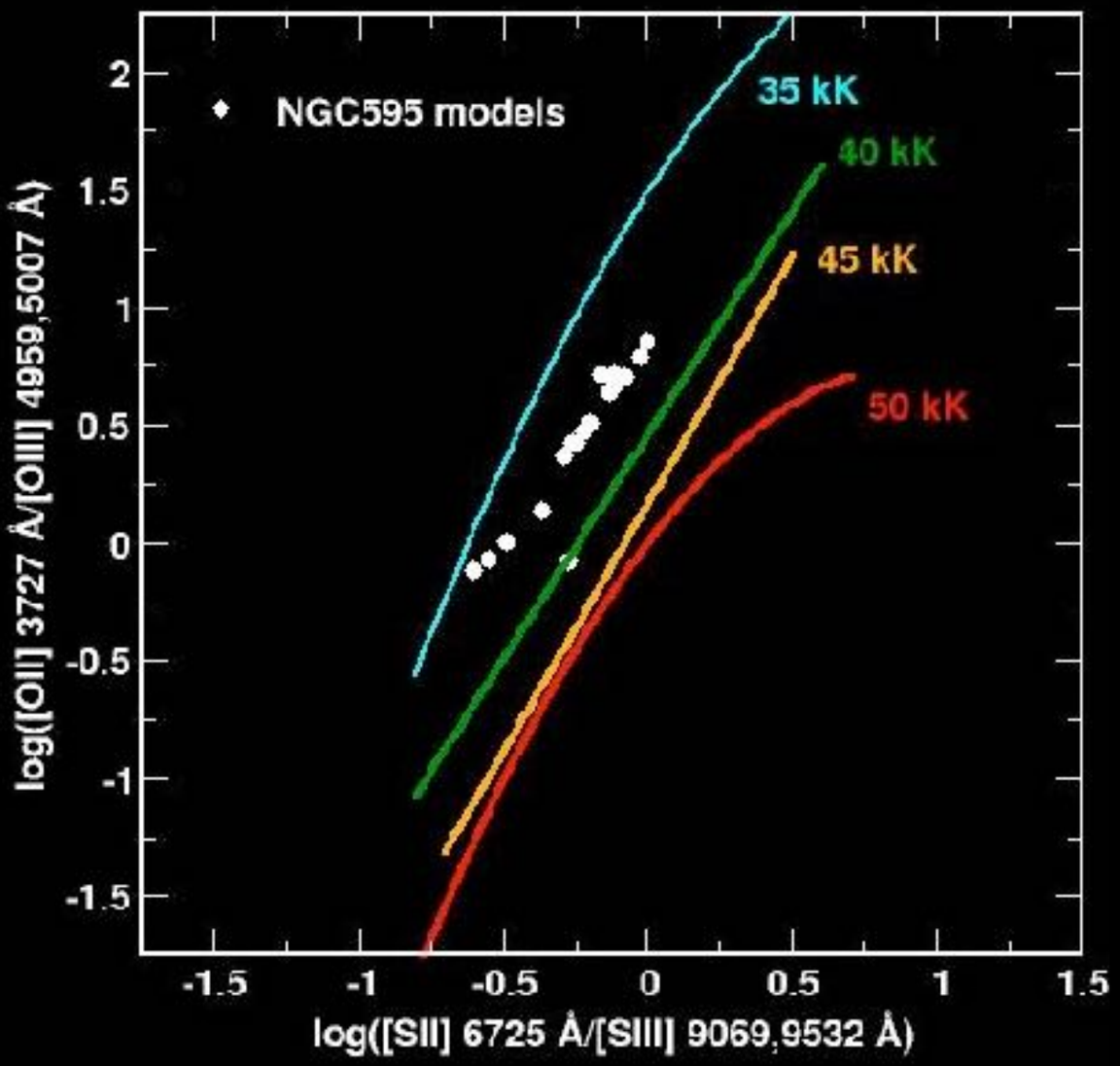
but the absolute calibration scale depends on the model stellar atmosphere, metallicity, and log U.

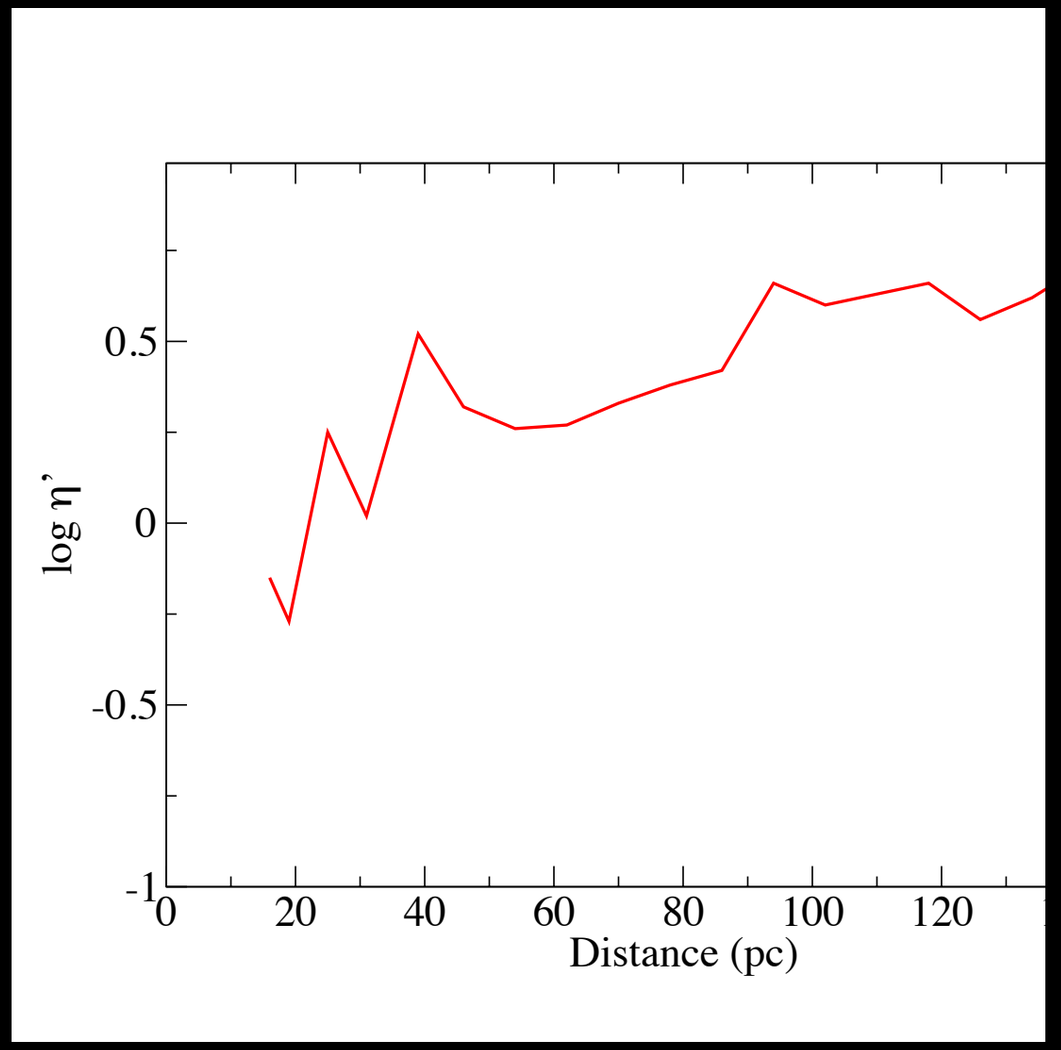
CAUTIONS WITH THE "SOFTNESS" PARAMETER



PMAS IFU optical observations of NGC595 (Relaño et al., 2010) and Spitzer images have been modelized to reproduce its optical and IR structure (Pérez-Montero et al., 2011)

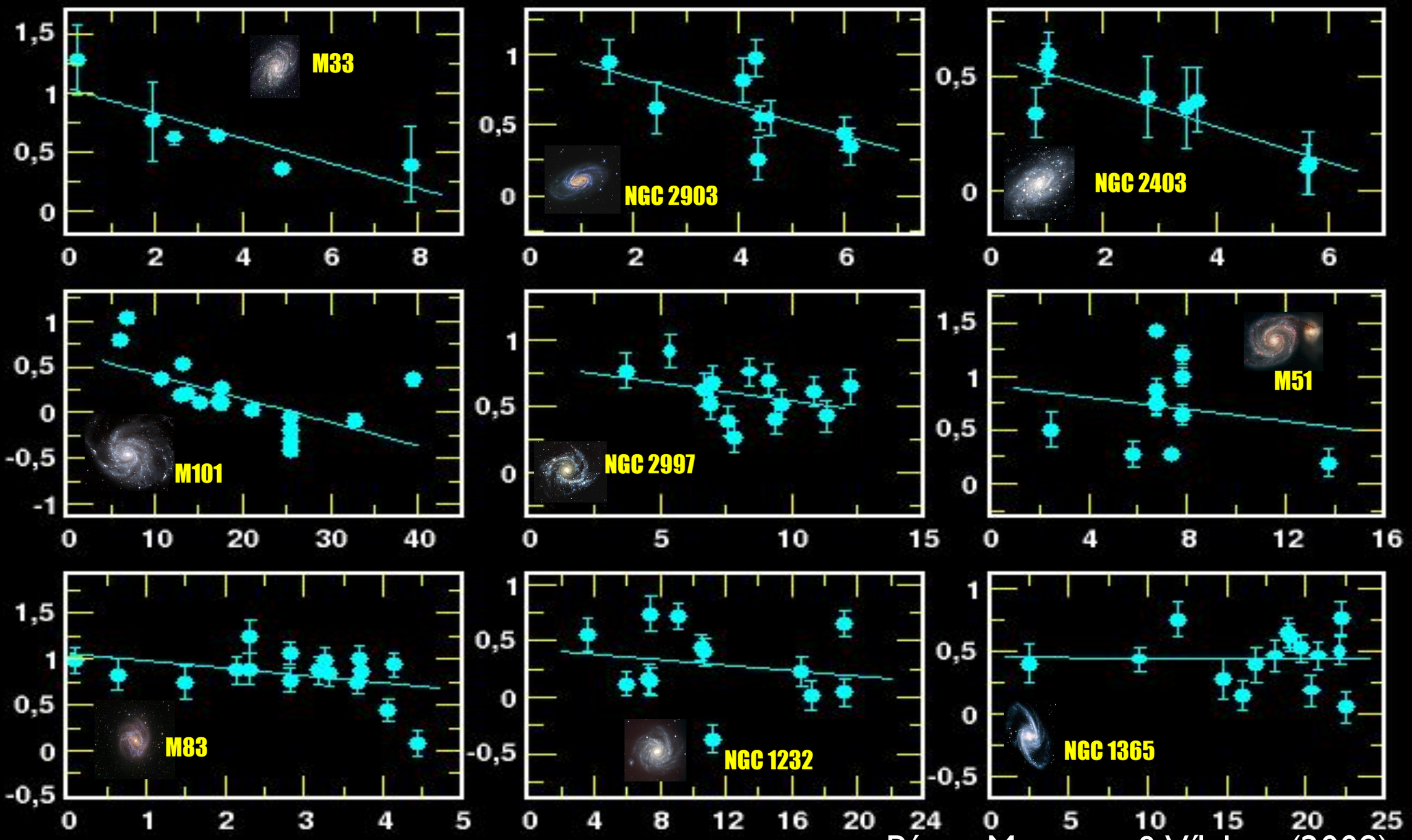
CAUTIONS WITH THE "SOFTNESS" PARAMETER





The models of the gas give T* consistent with the stellar cluster (39200K) although the radial profile of the softness parameter increases according to models

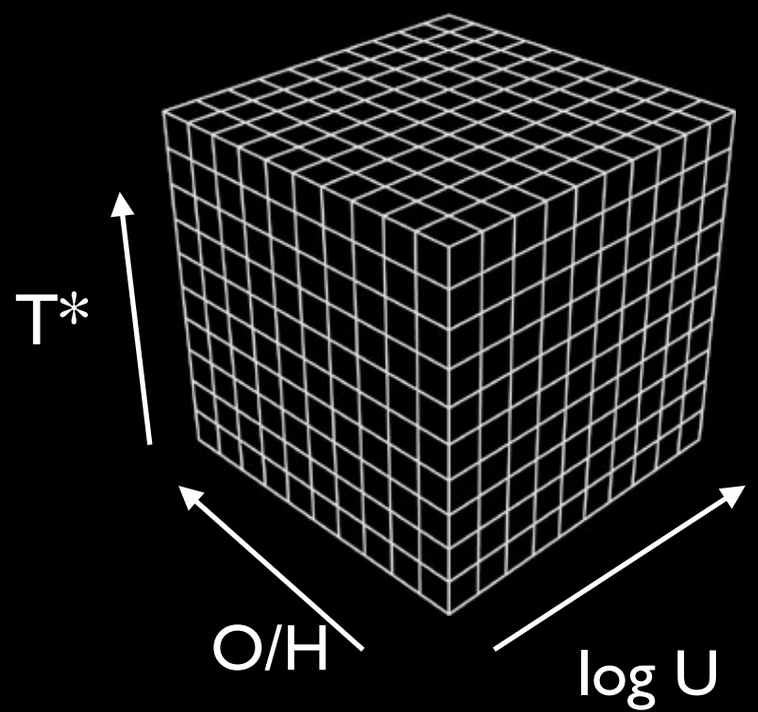
SPIRAL DISKS GRADIENTS OF η



Pérez-Montero & Vílchez (2009)

Are the observed radial decreasing of η in galaxies owing to a hardening of the ionizing stellar radiation?

A GRID OF MODELS TO DERIVE T*



We calculated a grid of models to derive U and T* from the lines of the softness parameter

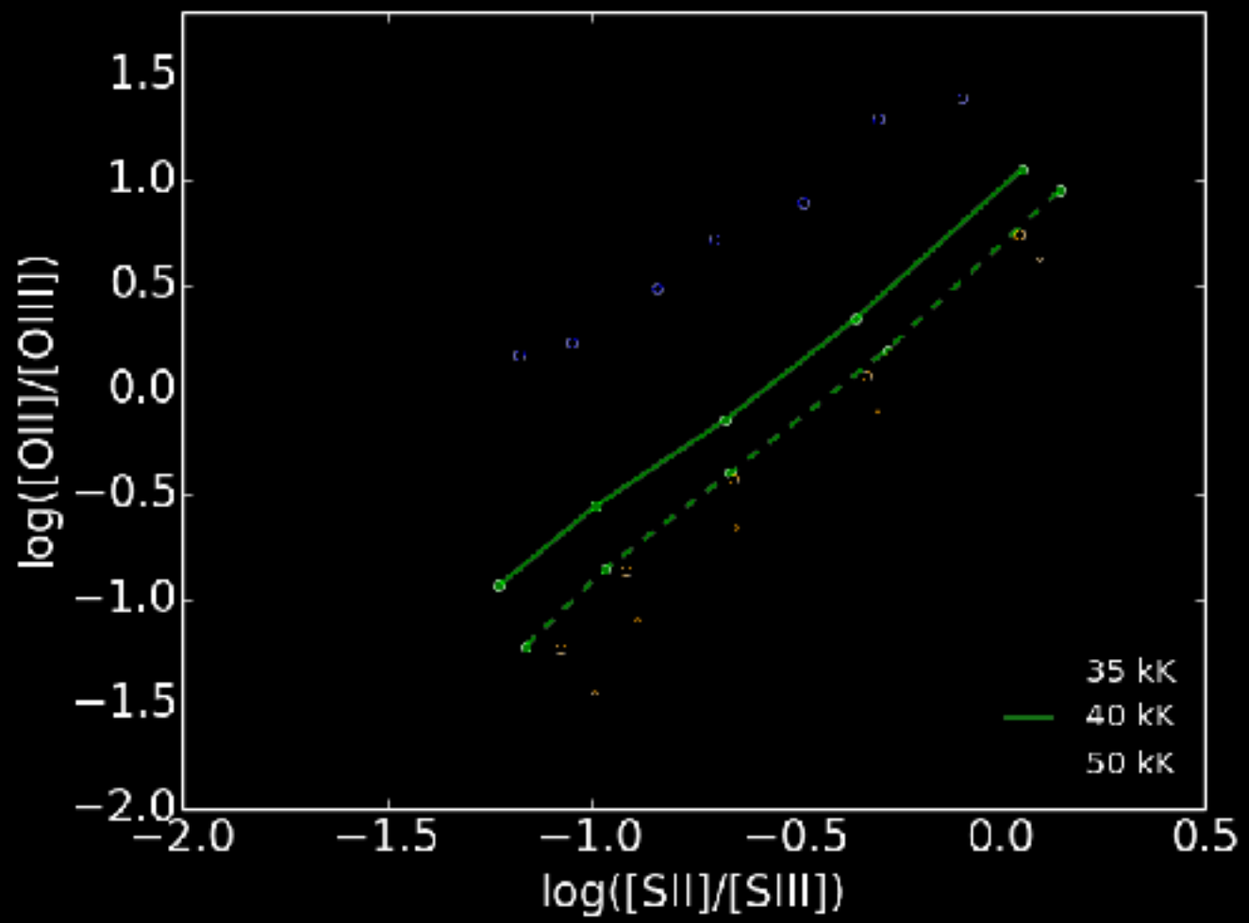
- Cloudy v. 17.00 (Ferland et al. 2017)
- **WM-Basic single-star atmospheres (Pauldrach2002)(same Z as the gas,**
- **- Constant density**

- Radiation-bounded geometry
- All elements scaled to O, except N
- Standard MW dust-to-gas ratio
- Variation of input parameter:
  - 12+log(O/H): [7.1, 8.9] 0.3bin
  - T*): [30,000,55,000]]
  - log U: [-3.5,-1.5] 0.5bins

This gives a total of 280 models

METALLICITY DEPENDENCE

The lines of equal U or T* depend strongly on the metallicity of the model. The first step then is to choose or interpolate the models to be applied to a dataset.



Metallicity is key to provide accurate values. When O/H is known the used grid is interpolated.

THE HII-CHI-mistry Teff CODE

The HCm-Teff code calculates T* and U comparing the input emission-line fluxes of [OII], [OIII], [SII], and [SIII] with the values in the models as the chi2-weighted means of the values of the grid.

$$T_{*f} = \frac{\sum_i T_{*i}/\chi_i^2}{\sum_i 1/\chi_i^2}$$

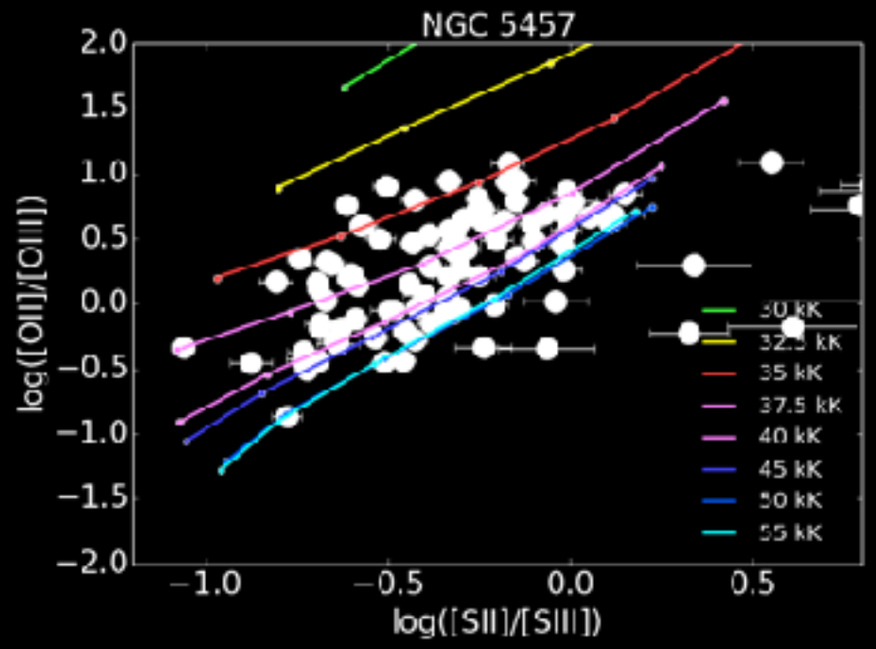
$$\log(U)_f = \frac{\sum_i \log(U)_i/\chi_i^2}{\sum_i 1/\chi_i^2}$$

Errors are calculated as the standard deviation of the weighted distributions. In addition the observational errors of the lines are considered in a monte-Carlo iteration that is later added to final error balance.

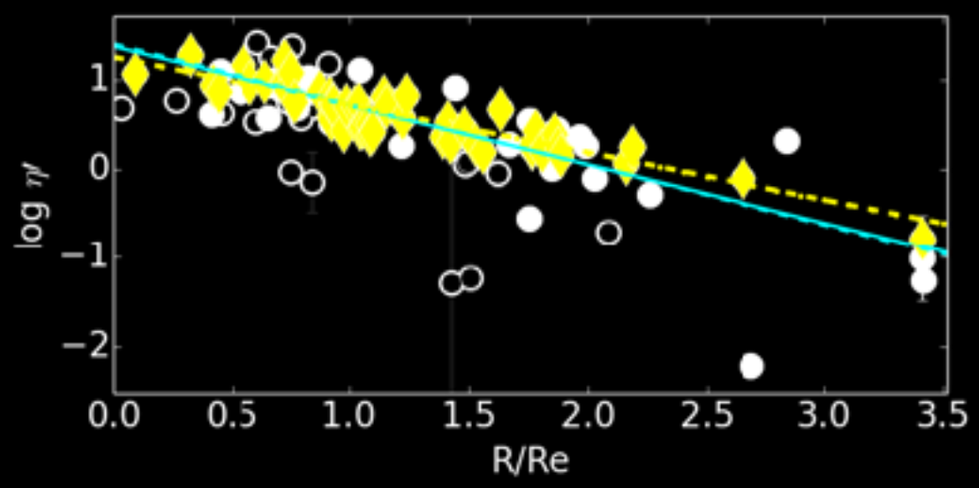
All versions of HCm can be retrieved from the HII-CHI-mistry webpage !!!

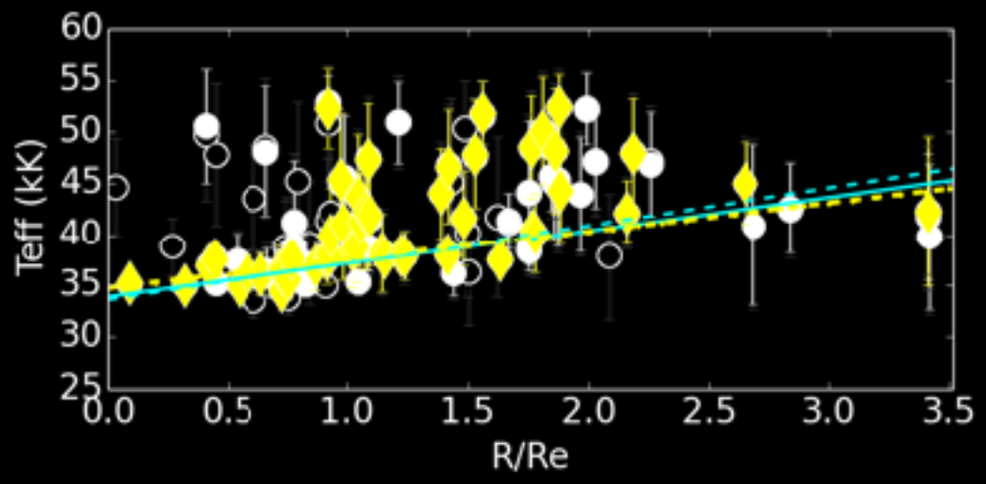
HCm Teff

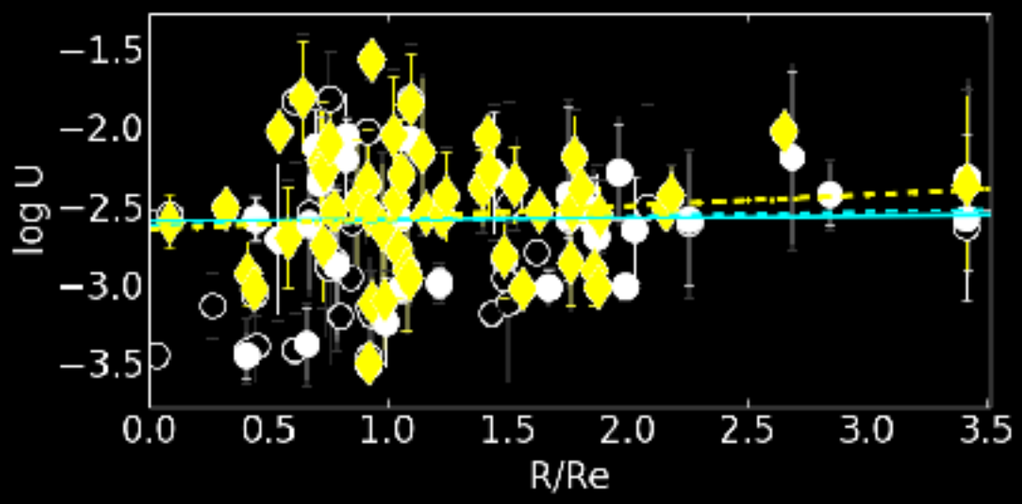
STUDY OF GRADIENTS IN M101





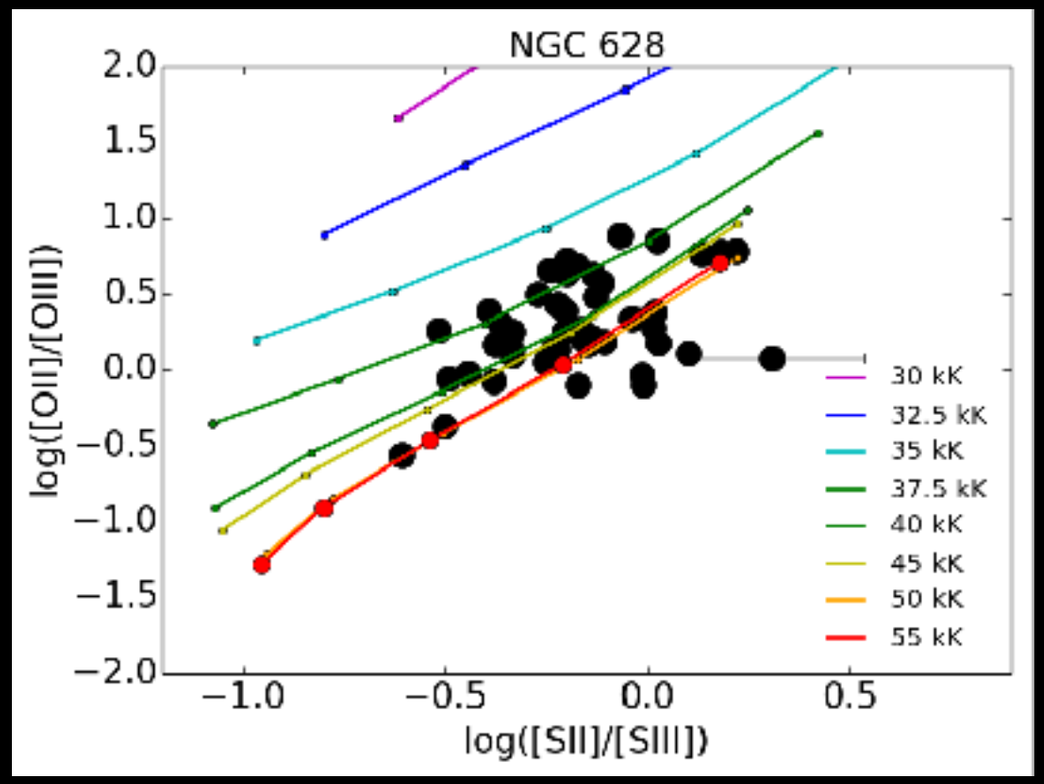


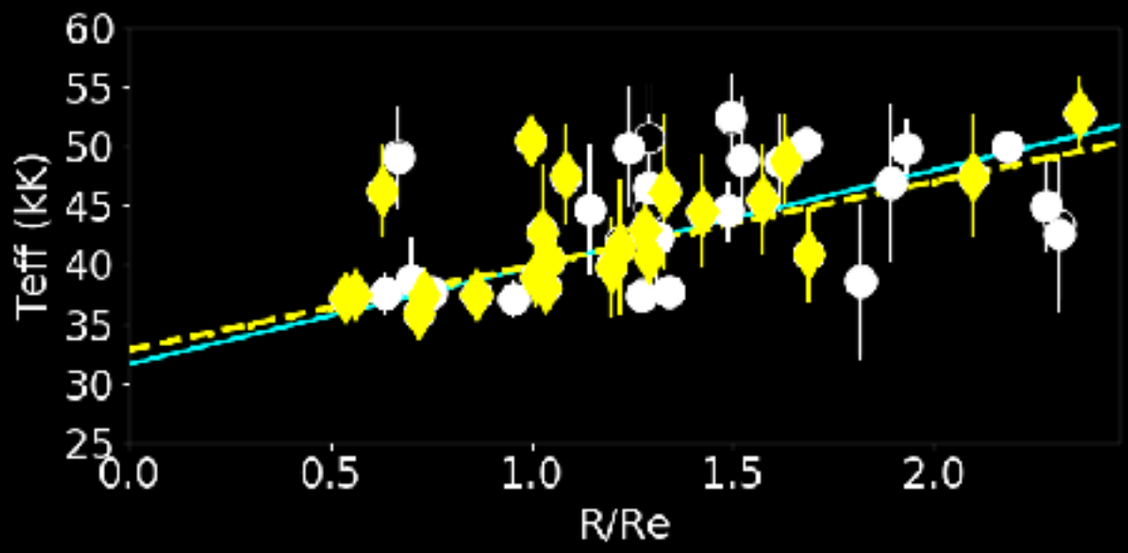




STUDY OF GRADIENTS IN M74



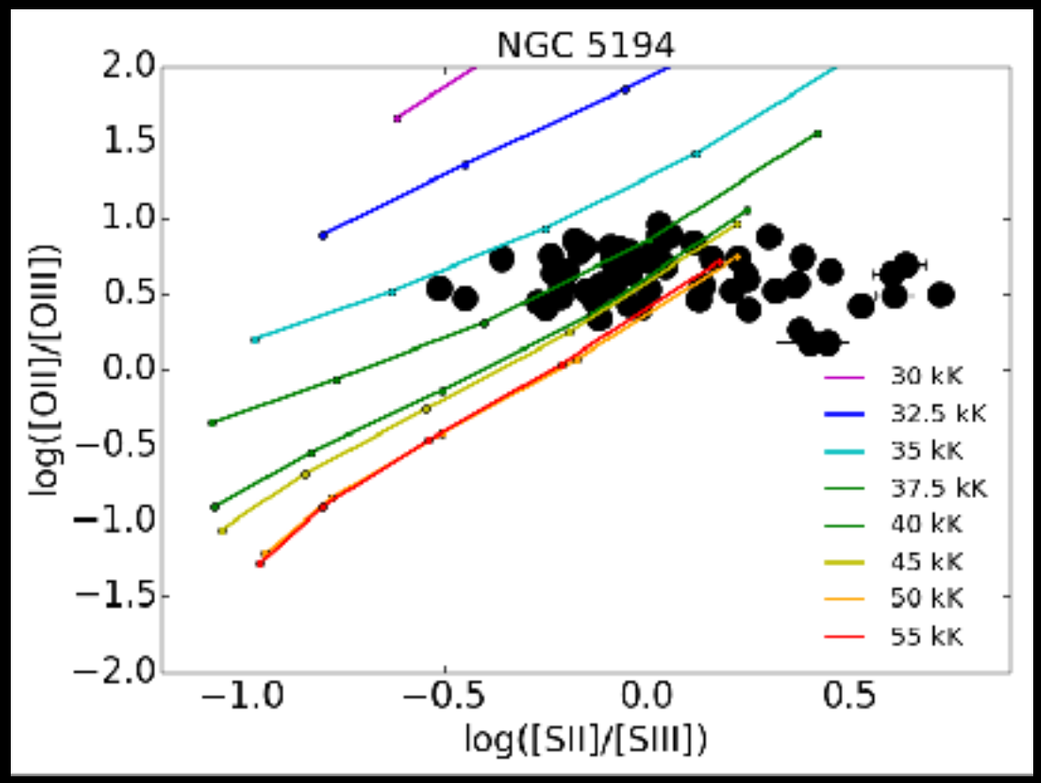


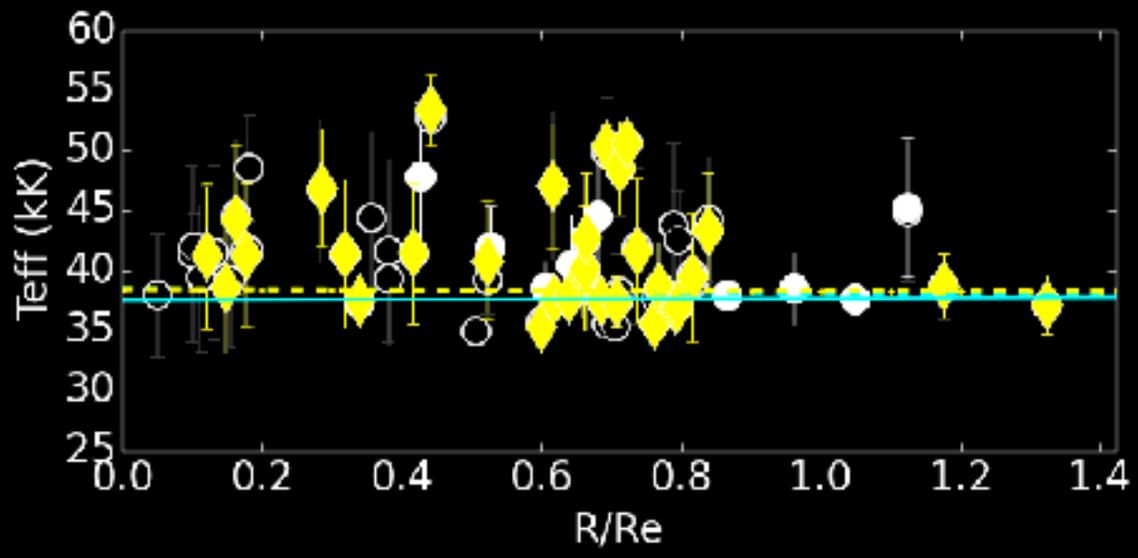


Pérez-Montero et al (2019)

STUDY OF GRADIENTS IN M51



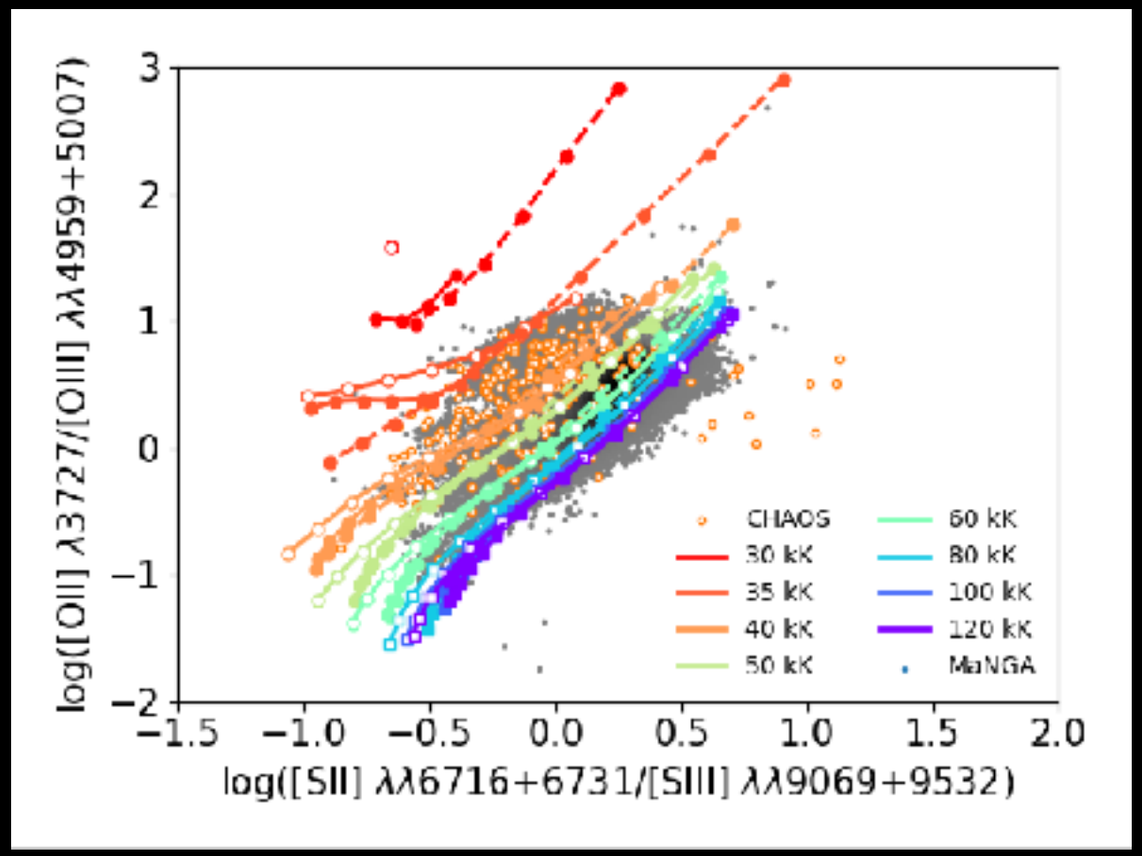


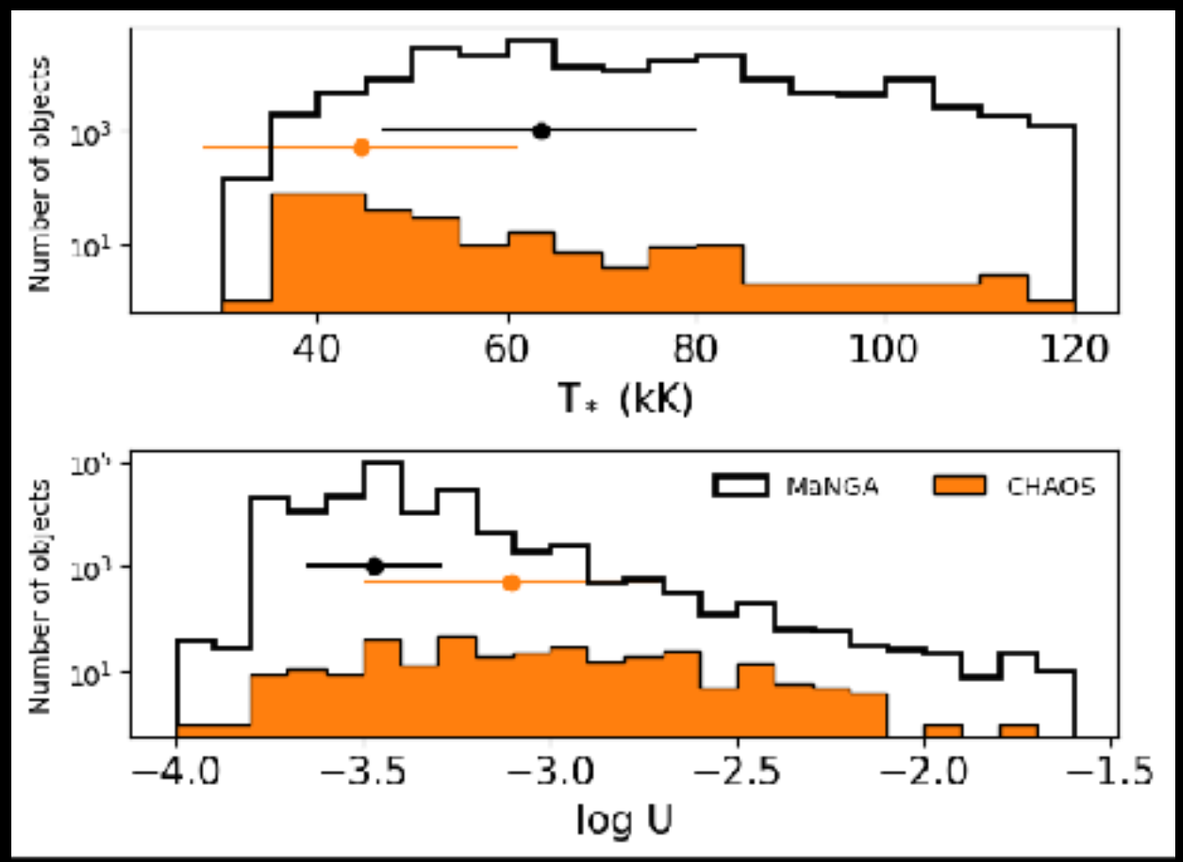


Pérez-Montero et al (2019)

THE IMPORTANCE OF GEOMETRY

More than 60% of HII regions in MaNGA would have T* > 60 kK, contrary to CHAOS.
This fraction is hugely reduced when replacing [SII] with other low-excitation line less affected by DIG.

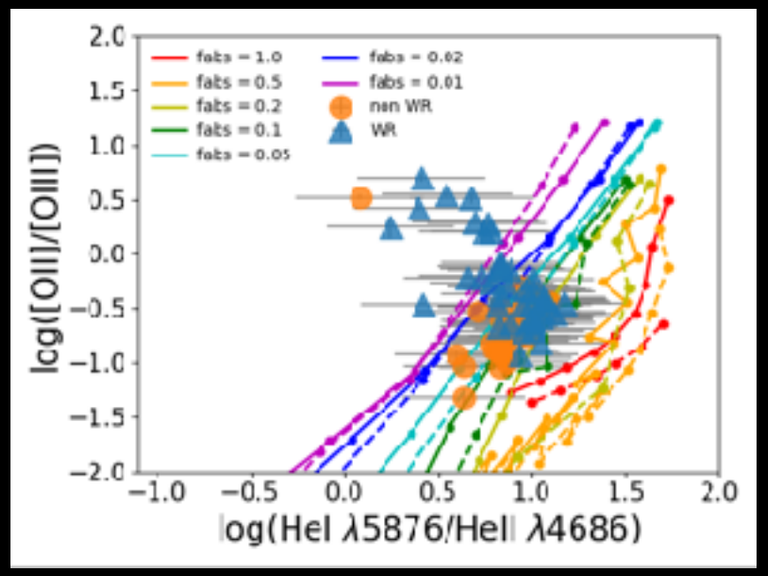


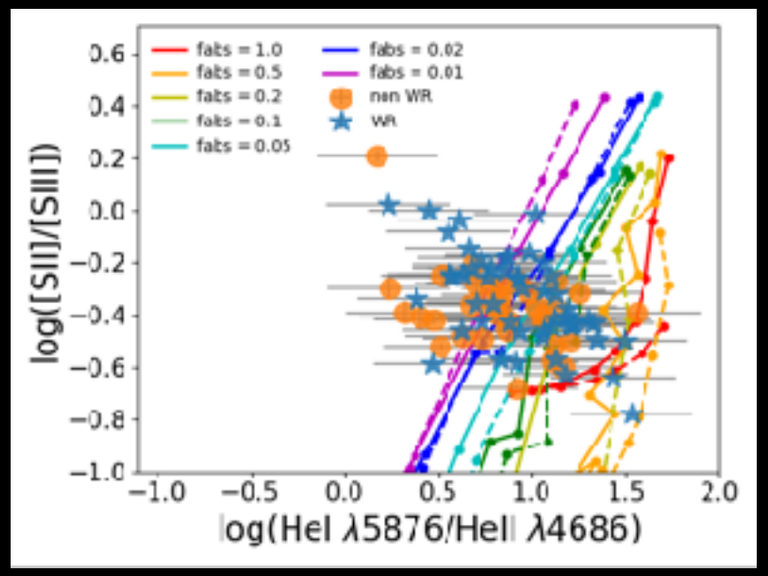


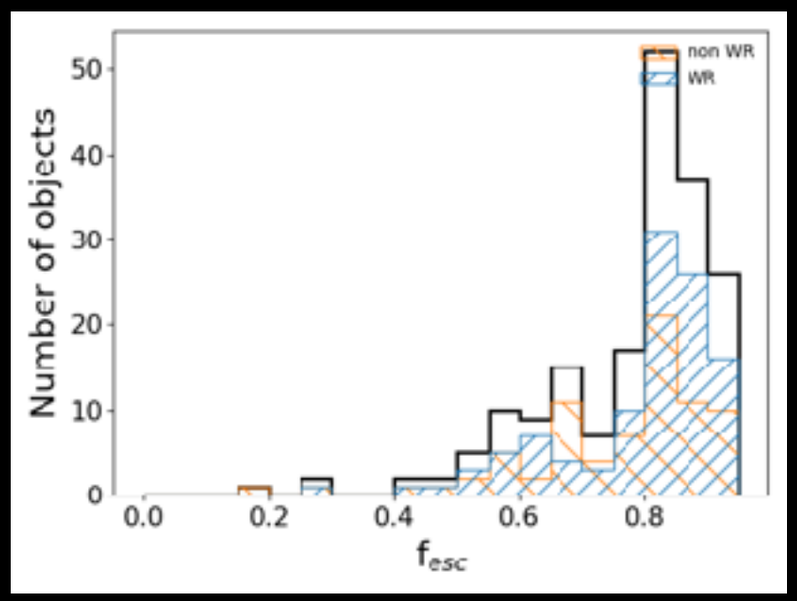
Pérez-Montero et al (2023a)

USING THE DIAGRAM FOR PHOTON ESCAPE FRACTION

Pérez-Montero et al (2020)



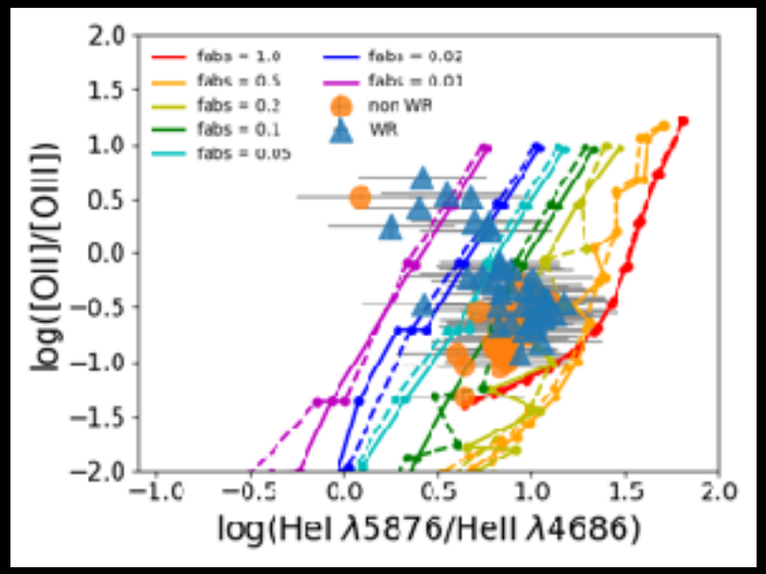


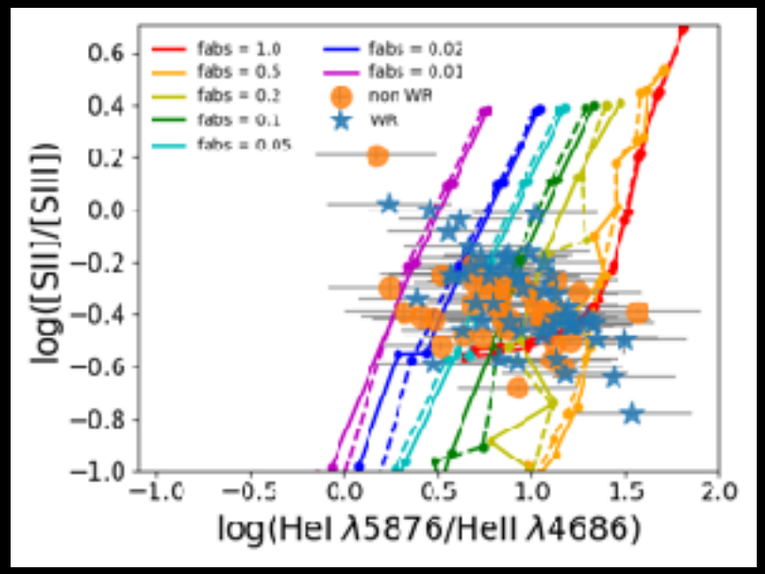


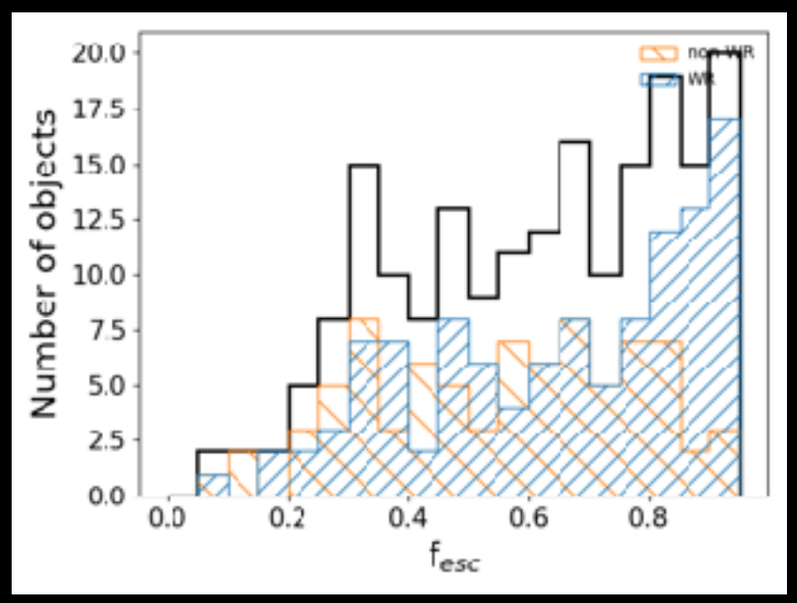
We can calculate f_esc from models using other line ratios.
The analysis of 129 HeII emitters in SDSS using BPASS v.2.1 models assuming Z* = Zg yields a mean value of 79% for both Wr and non WR objects.

USING THE DIAGRAM FOR PHOTON ESCAPE FRACTION

Pérez-Montero et al (2020)



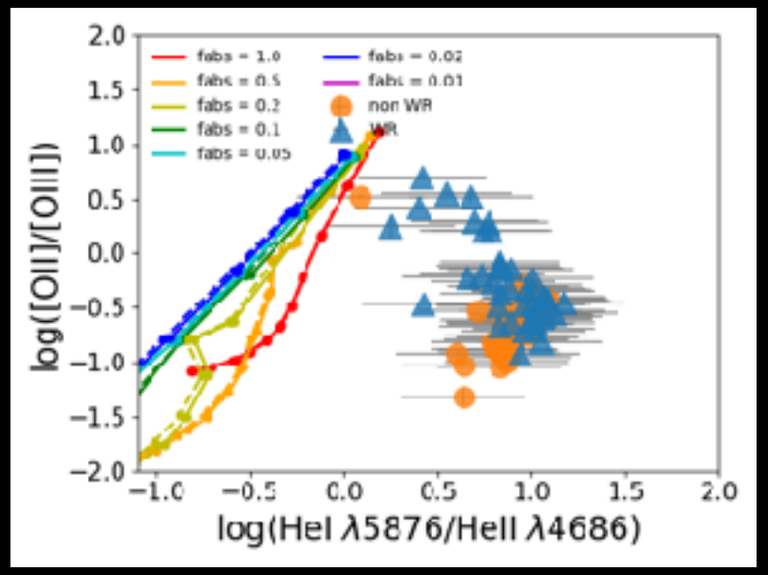


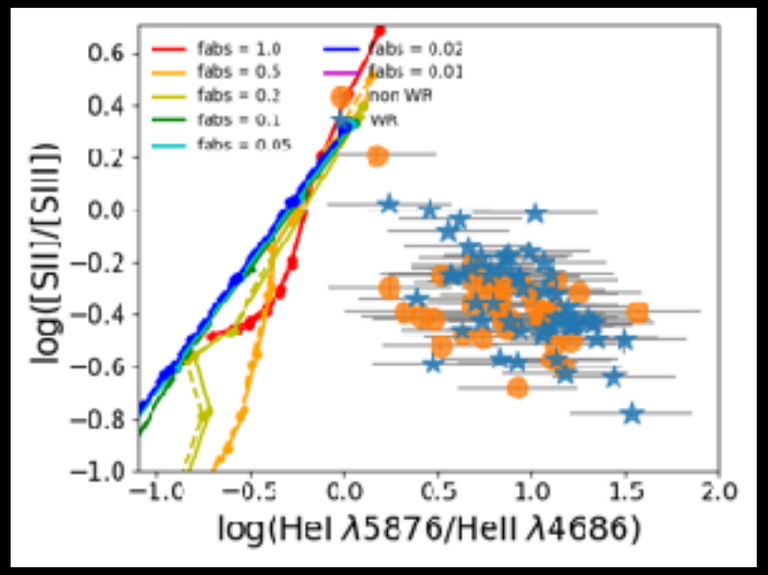


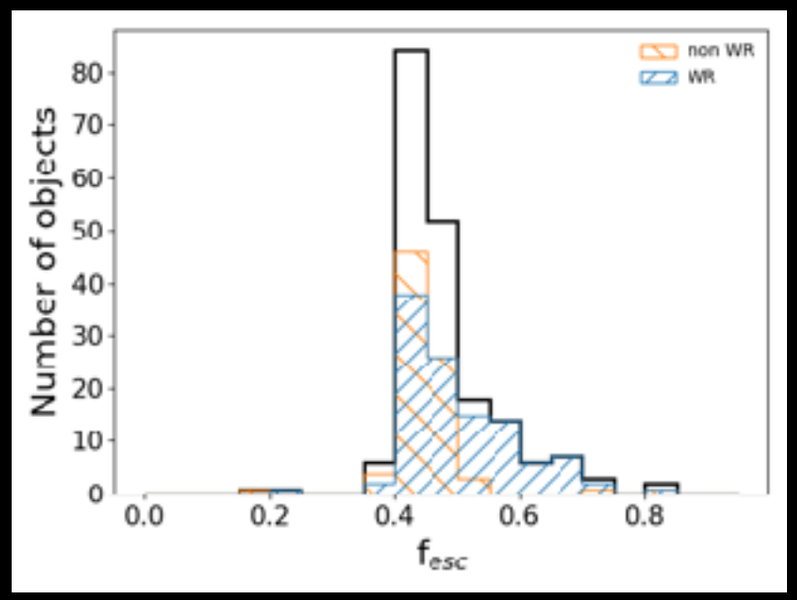
But this is sensitive to the assumed SED. For very-low Z stars (Z = 1e-5), the mean escape fraction for this sample is reduced to 62%.

USING THE DIAGRAM FOR PHOTON ESCAPE FRACTION

Pérez-Montero et al (2020)

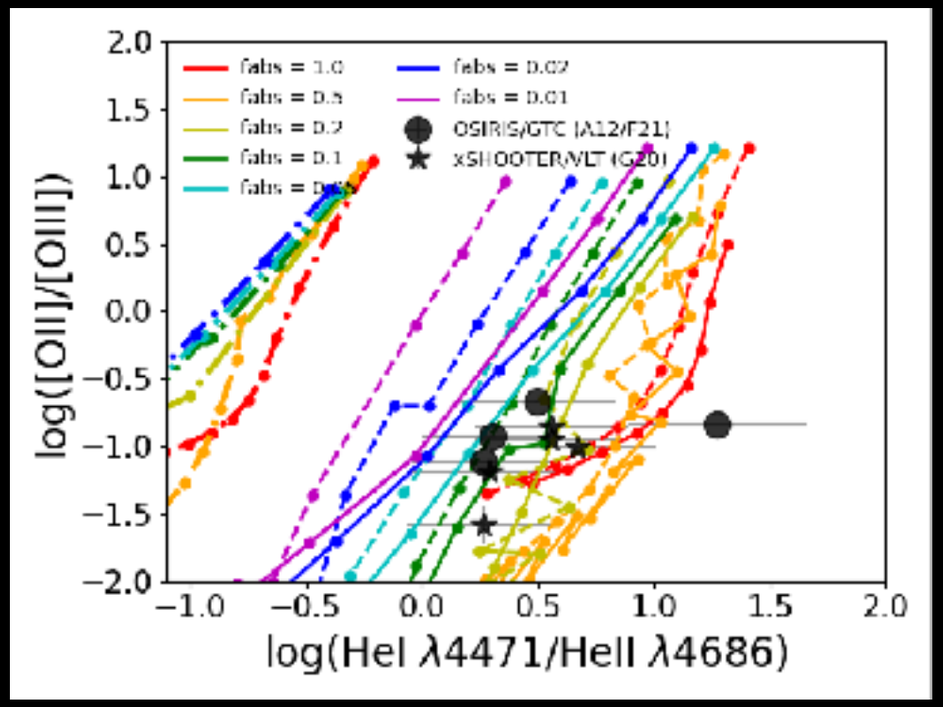


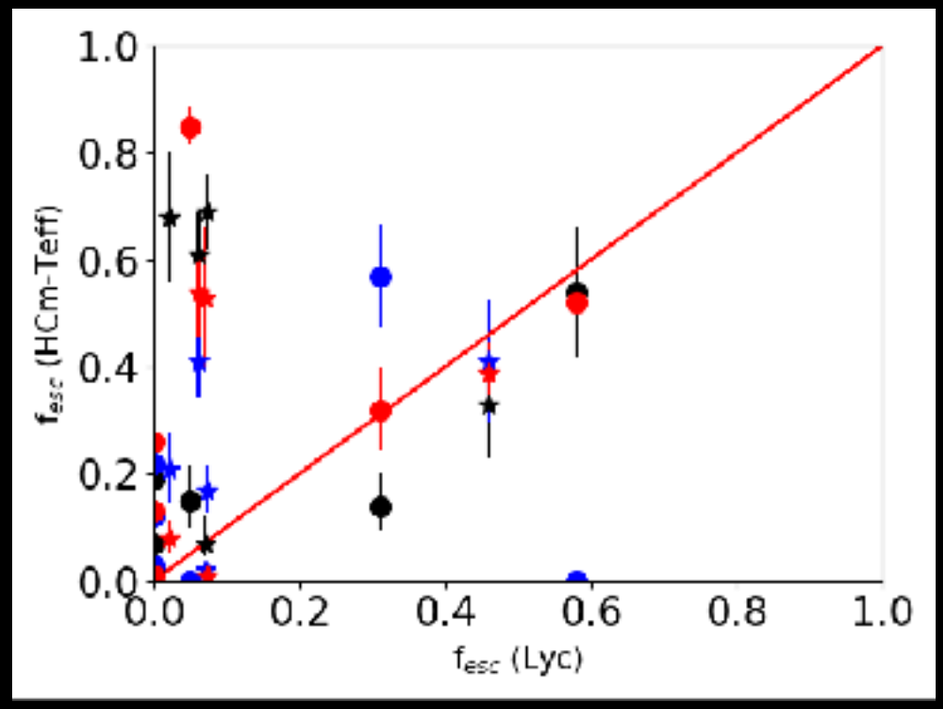




… and assuming SEDs for blackbody at T* = 1e5K)thought to be equivalent to PopIII stars= the mean fraction is reduced to 48%.

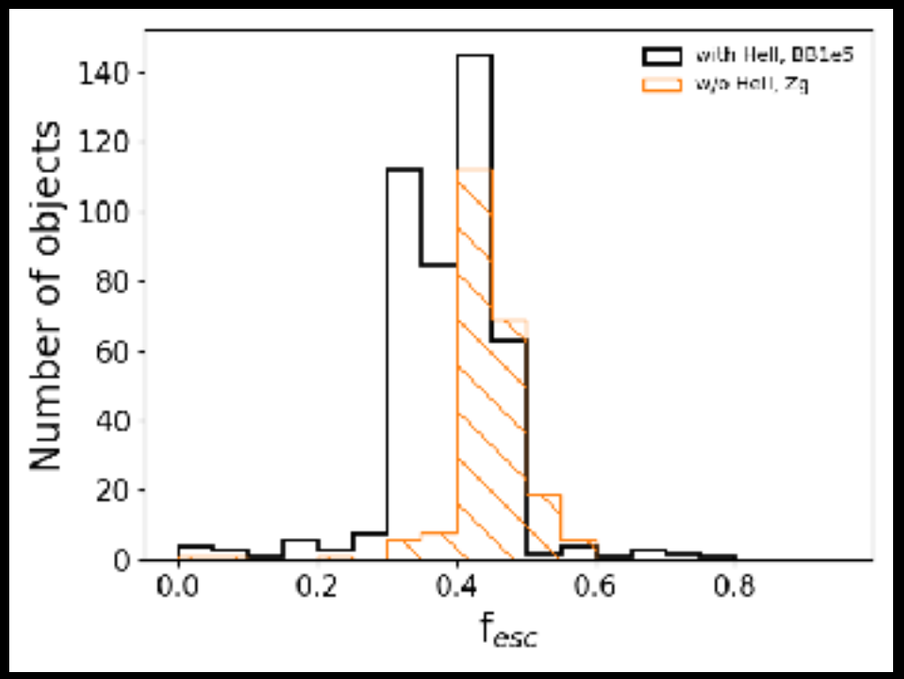
ANALYZING DEEP OPTICAL OBSERVATIONS OF GP

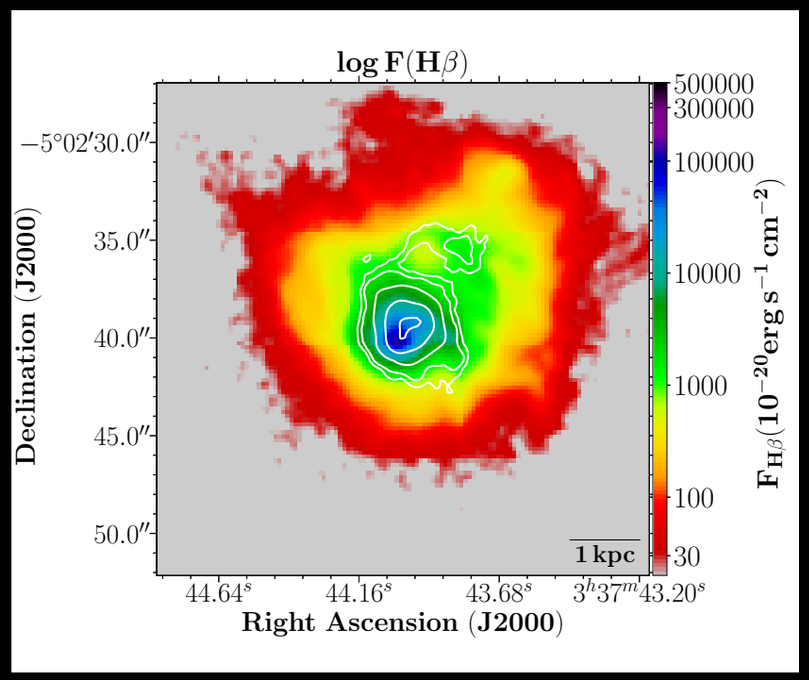




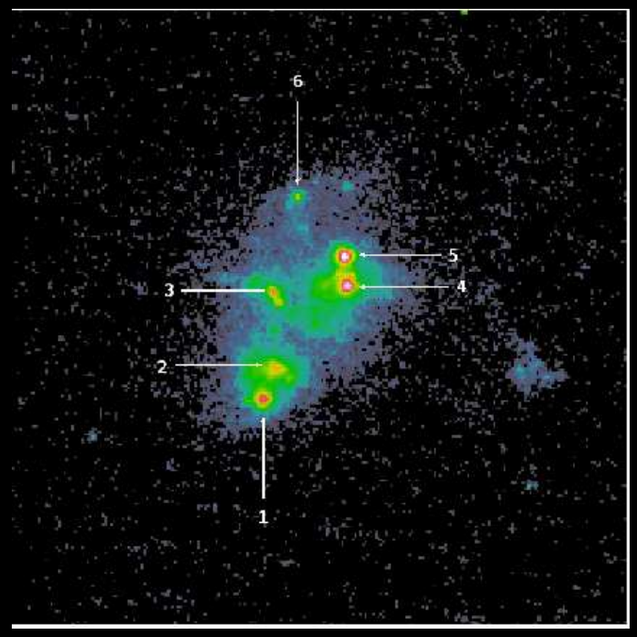
HeII emission has been retrieved from very deep spectroscopy in some GPs (OSIRIS/GTC: Amorín+12, Fernández+21 and xSHOOTER/VLT: Guseva+20). The derived escape fractions can be compared with data from Ravindranath+20, but the agreement is very dependent on the assumed Z in the stars.

SPATIALLY-RESOLVED HeII EMITTERS





Analyzing MUSE data from SBS0335-052, escape fraction in spaxels with nebular HeII emission is consistent (~40%) with the rest of the galaxy only assuming PopIII stars (Kehrig et al in prep.)



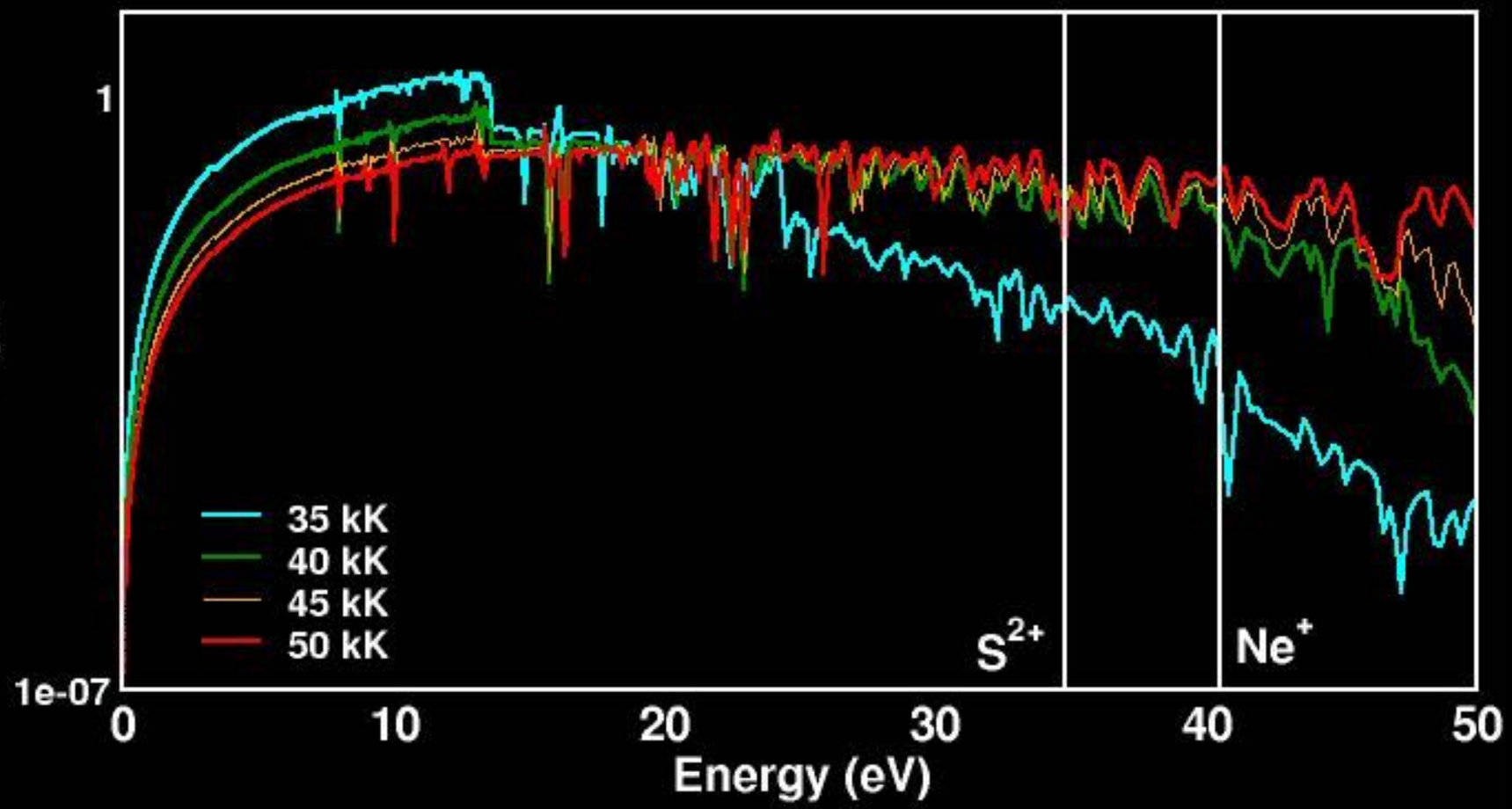
THE STEPHAN QUINTET



Source: NASA Chandra observatory. Combined infrared taken by JWST and X-ray taken by Chandra image of the compact group of Stephan quintet

THE IR "SOFTNESS" PARAMETER

WM-Basic, log(g)=4.0, [Z] = -0.3



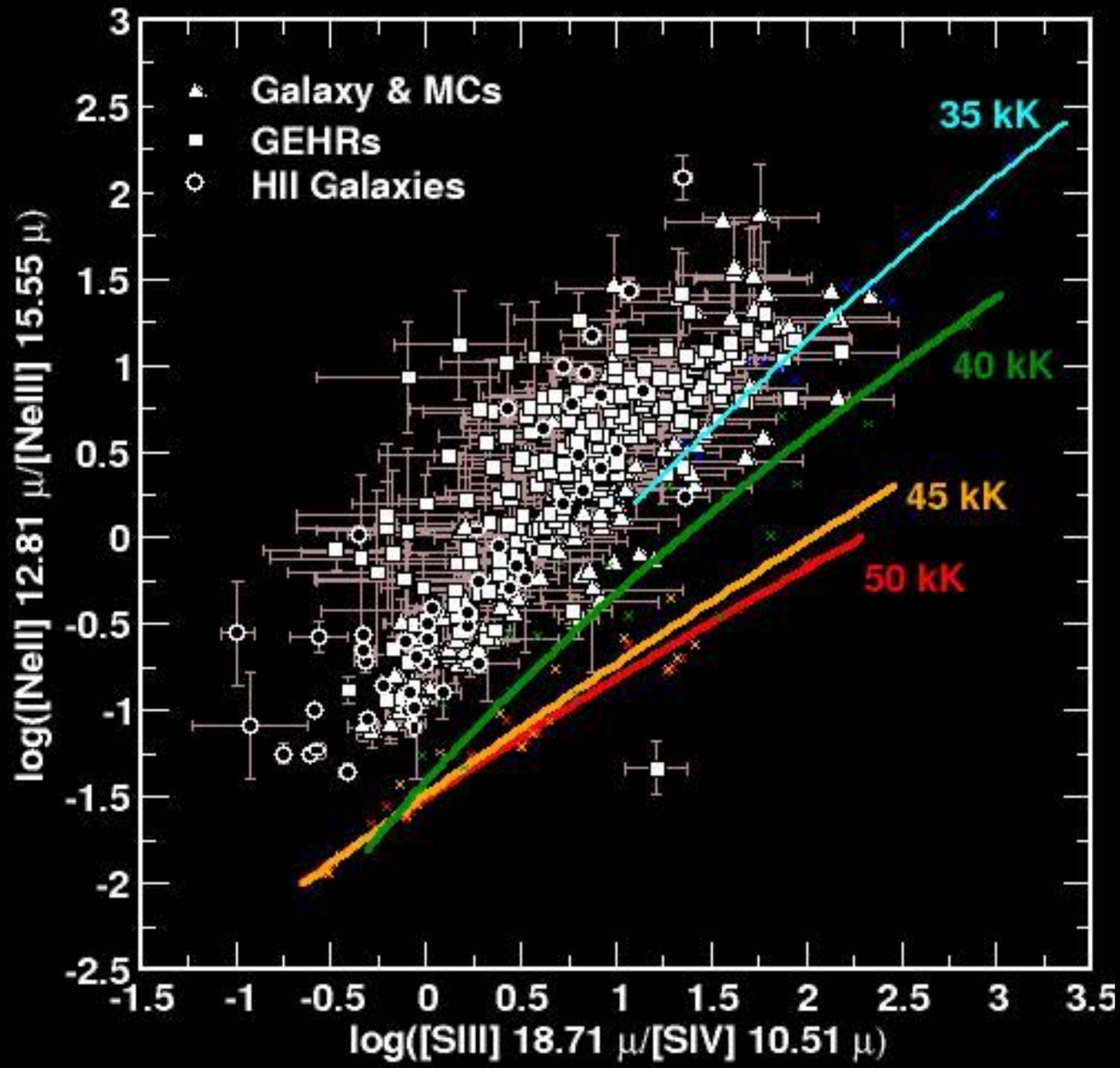
$$\eta = \frac{Ne^{+}/Ne^{2+}}{S^{2+}/S^{3+}} = \frac{[NeII]/[NeIII]}{[SIII]/[SIV]} + o(Z) \propto \frac{Q(Ne^{+})}{Q(S^{2+})}$$

Morisset et al. (2004)

THE IR "SOFTNESS" DIAGRAM

However, as in the optical, models indicate ana additional dependence on U, so a 2D analysis is required to break the degeneracy.

WMBasic model stellar atmosph.

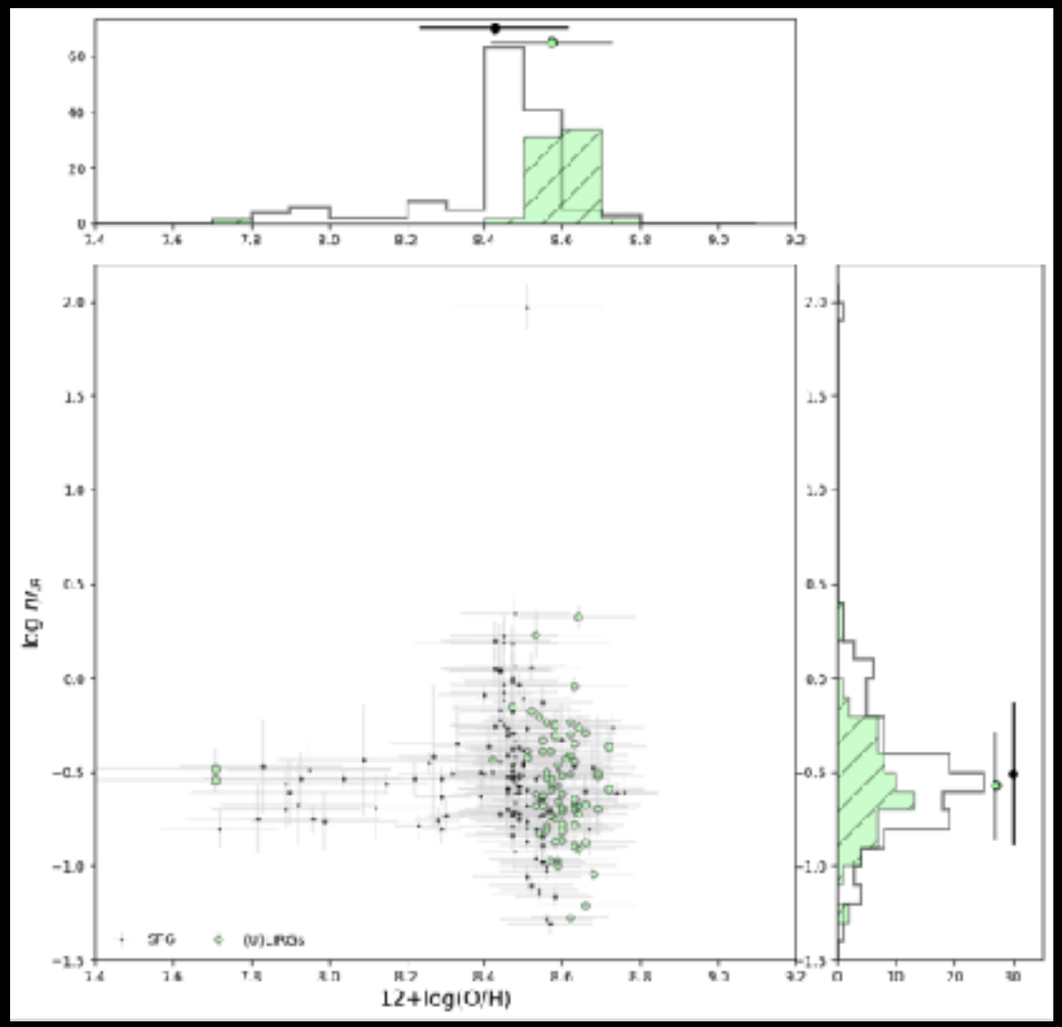


Pérez-Montero & Vílchez (2009)

SAMPLING NEW IR DATA WITH IDEOS

We compiled a new sample of IR data to re-evaluate the behavior of eta_IR including SFGs and ULIRGs for which we can derive IR metallicities.

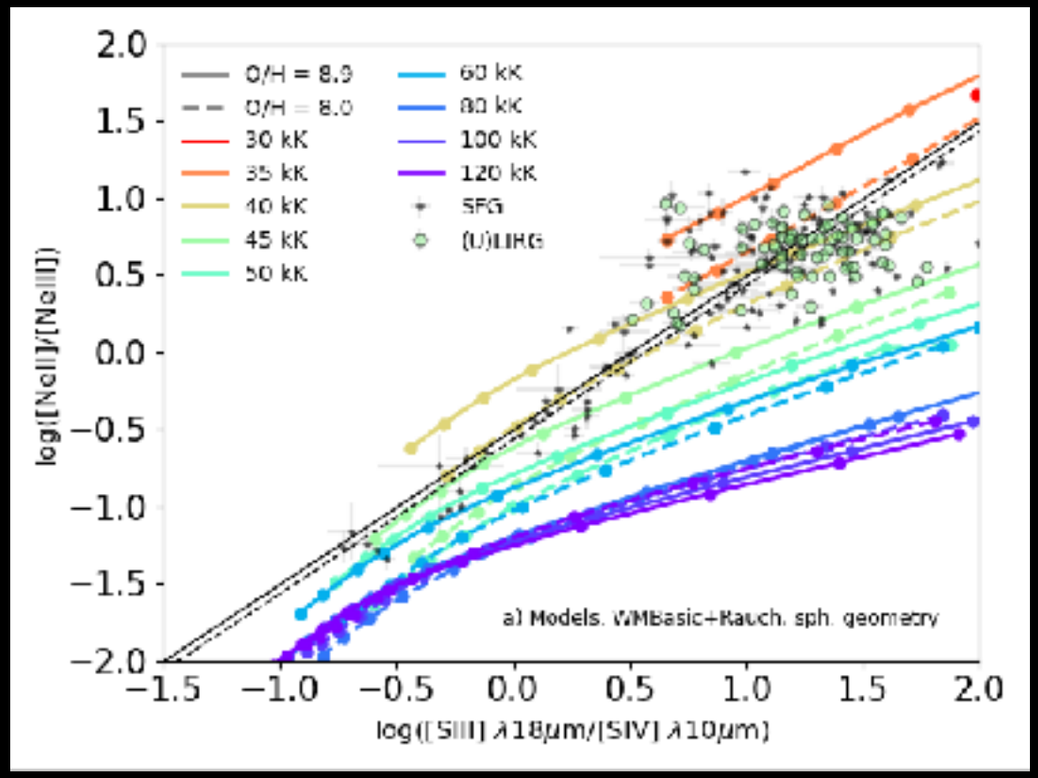
No significant difference is found between the average eta for SFGs and ULIRGs



Pérez-Montero et al (2024)

DEPENDENCE OF THE DIAGRAM ON MODELS

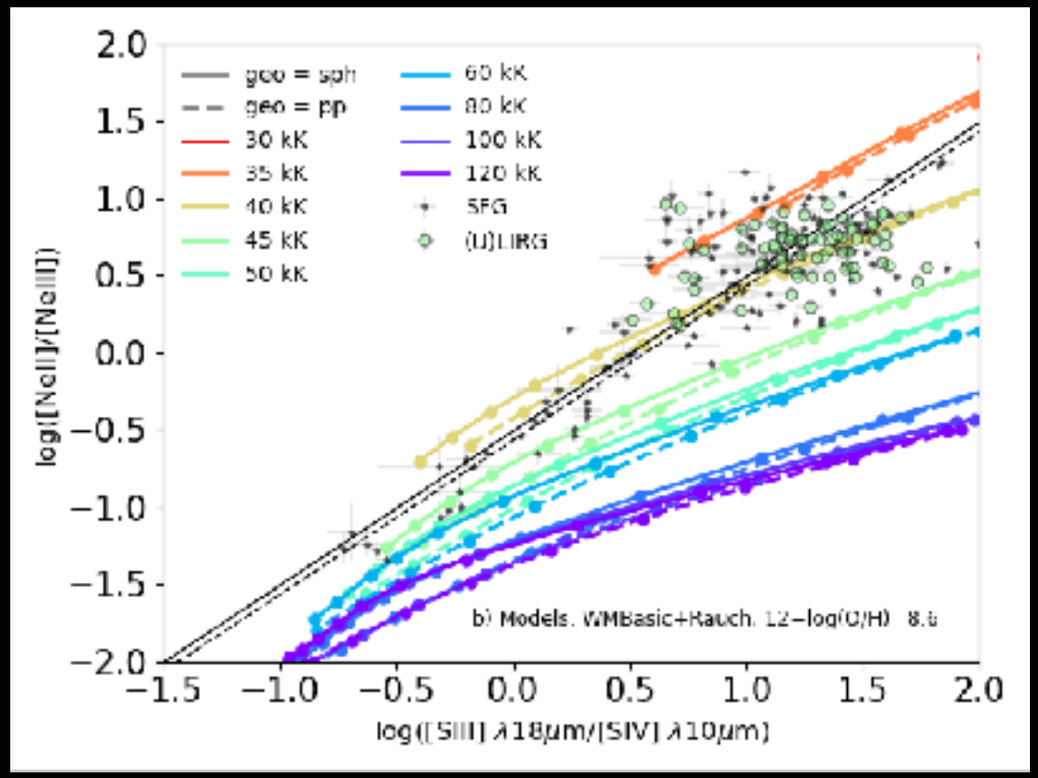
When compared with the grid of models in the diagram, the sequences match the data with no need of ionizing sources harder than massive stars nor neither for ULIRGs nor for the rest of SFGs



Pérez-Montero et al (2024)

DEPENDENCE OF THE DIAGRAM ON MODELS

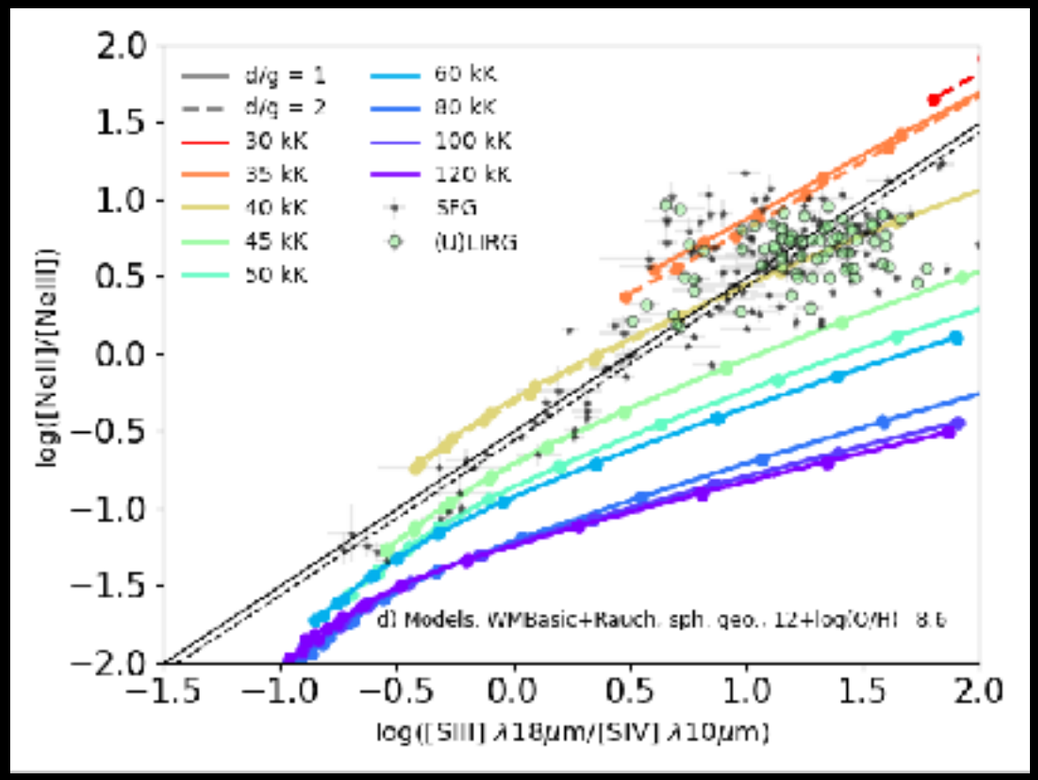
The geometry assume in the models does not seem to produce significant differences in the results, but photon leaking must be still checked.



Pérez-Montero et al (2024)

DEPENDENCE OF THE DIAGRAM ON MODELS

Regarding dust-to-gas mass ratio, possibly higher in ULIRGs, this neither implies large differences in the results.

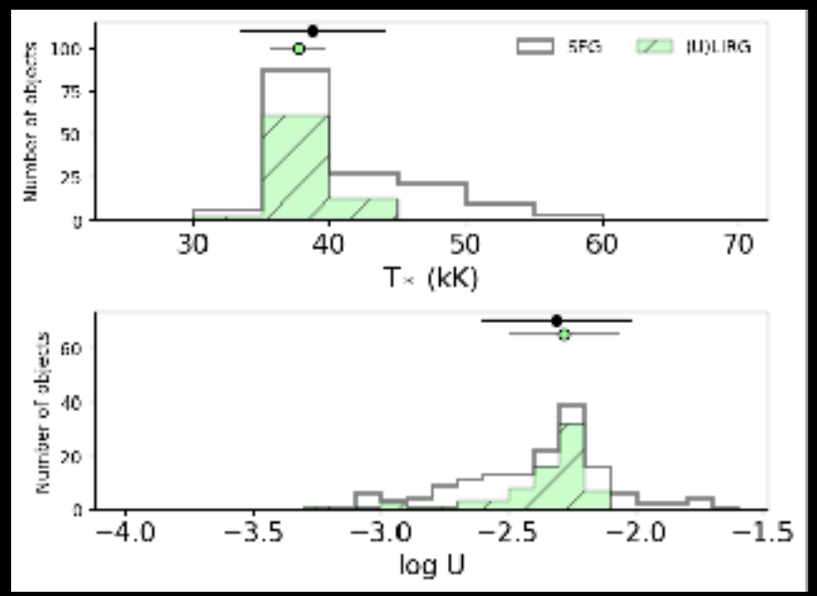


Pérez-Montero et al (2024)

APPLYING THE HCm-Teff-IR CODE

Table 1. Means and dispersions of the resulting T_* and log U values obtained from HCm-Teff for the subsamples of SFGs and (U)LIRGs analysed here under different assumptions of SED geometry (sph stands for spherical and pp for plane-parallel), or dust-to-gas ratio (a d/g_{MW} value is assumed if not specified). We also list the average metallicity for each set.

	SFG	ULIRG
N	228	75
12+log(O/H)	8.46 (0.23)	8.56 (0.18)
log Σ_{IR}	-0.51 (0.28)	-0.57 (0.28)
WM3 (30-60 kK)		
T_* (kK), pp	42.3 (3.8)	4..1 (..4)
log U, pp	-2.52 (0.29)	-2.51 (0.16)
T_* (kK), sph	39.9 (4.7)	38.0 (2.0)
log U, sph	-2.37 (0.27)	-2.36 (0.21)
T_* (kK), sph, $2d/g_{MW}$	41.8 (4.7)	39.8 (..6)
log U, sph, $2d/g_{MW}$	-2.36 (0.32)	-2.42 (0.17)
WM-Basic (30-60 kK) + Basic (80-120 kK)		
T_* (kK), pp	53.1 (3.0)	5..8 (4.4)
log U, pp	-2.62 (0.27)	-2.70 (0.15)
T_* (kK), sph	48.1 (8.8)	43.6 (3.9)
log U, sph	-2.47 (0.25)	-2.45 (0.19)
T_* (kK), sph, $2d/g_{MW}$	51.4 (9.9)	48.2 (4.5)
log U, sph, $2d/g_{MW}$	-2.46 (0.26)	-2.51 (0.15)
BB (30-100 kK)		
T_* (kK), sph	51.3 (8.1)	51.1 (10.0)
log U, sph	-2.01 (0.52)	-2.15 (0.31)
T_* (kK), pp	52.1 (8.4)	5..5 (5.0)
log U, pp	-2.61 (0.27)	-2.71 (0.15)



Pérez-Montero et al (2024)

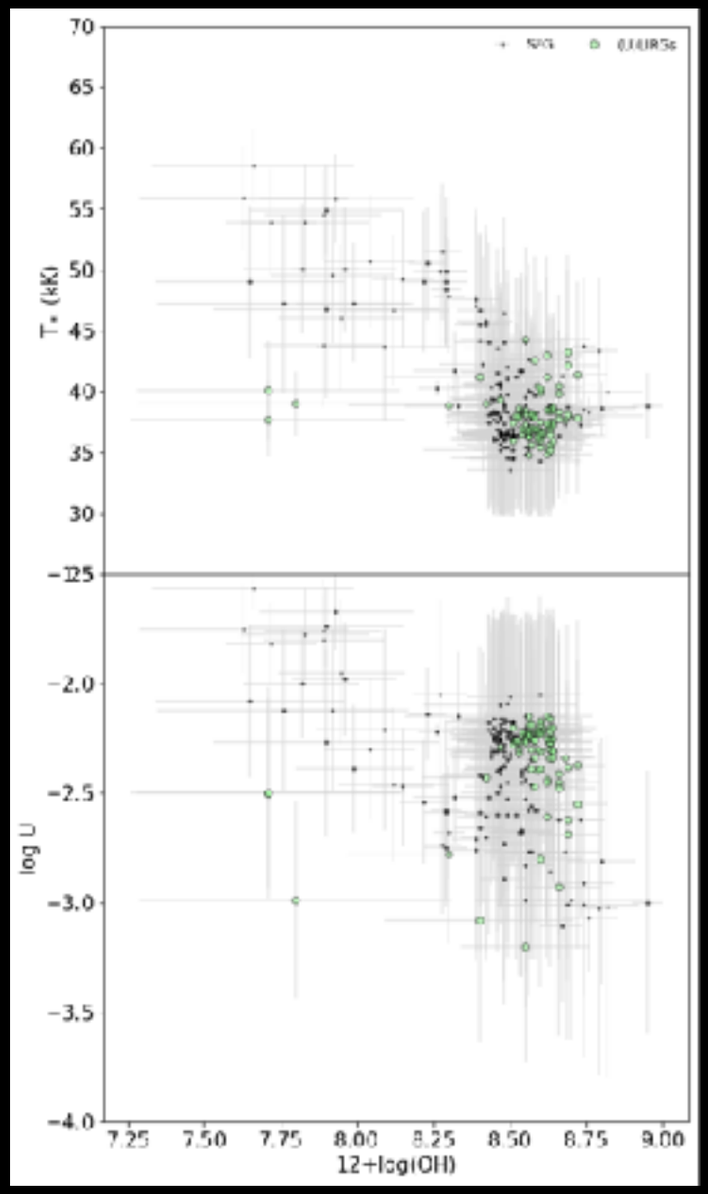
An adapted version of HII-CHI-mistry-Teff for IR lines has been prepared and can be retrieved from the HCm web.

The application of the code to the sample confirm that ULIRGs and SFGs present similar T* within the errors, with possible slightly lower U values for ULIRGs.

HCm Teff

RELATION OF T* WITH METALLICITY

However, large differences are found when the relation with Z is explored, as T* correlates with O/H in SFGs, unlike ULIRGs, for which no correlation at all is observed.
This could be indicative that the T^values obtained for ULIRGs and the presence of dust grains around the stellar clusters is playing a relevant role.



Pérez-Montero et al (2024)

FUTURE WORK

*We plan to enlarge the code to explore the shape of the SED in AGNs, taking advantage of the very high ionization emission lines in the IR

*The possibility of photon leaking and how high excitation IR lines can be exploited can also be incorporated both for SFGs and AGNs

*We plan to extend the study of radial variations of T^using both optical and IR lines in large surveys, such as MaNGA

SUMMARY AND CONCLUSIONS

The softness diagram can be used to derive T in massive stellar clusters but it presents additional dependence on Z, U and other conditions.

* HCm-Teff allows to extract U and T^from the observational information from the lines, helping to clarify if the radial decreasing of eta can be interpreted as a hardening of the field of radiation.

*The diagram also depends on geometry so it can be used to derive the fraction of escaping ionizing photons. The code is adapted to be used as a function of observed different ratios such as HeI/HeII or CIII]/CIV].

*Using IR lines confirms that massive stars are the main source of ionization and that ULIRGs are not ionized by a harder SED.



This research has been funded by grants PID2022-136598NB-C31, C32, and C33

The wokshop has been funded by grant PID2019-107408GB-C41

all grants are funded by MCIN/AEI/10.13039/501100011033 and by "ERDF A way of making Europe"

